Coordination Chemistry Reviews 255 (2011) 1159–1178

Contents lists available at ScienceDirect

Coordination Chemistry Reviews

journal homepage: www.elsevier.com/locate/ccr

Review

Molybdenum enzymes in bacteria and their maturation

Axel Magalon[a,*], Justin G. Fedor[b], Anne Walburger[a], Joel H. Weiner[b,*]

[a] Laboratoire de Chimie Bactérienne, Institut de Microbiologie de la Méditerranée, Centre National de la Recherche Scientifique, Marseille, France
[b] Department of Biochemistry, School of Molecular and Systems Medicine, Faculty of Medicine and Dentistry, University of Alberta, Edmonton, Alberta, Canada

Contents

ARTICLE INFO

Article history:
Received 24 September 2010
Accepted 19 December 2010
Available online 11 January 2011

ABSTRACT

Molybdenum pterin cofactor-containing enzymes exist in all domains of life and their importance is exemplified by their ubiquity, their roles in metabolic diversity and global geochemical cycles. In the prokaryotic enzymes the pterin cofactor coordinating the molybdenum/tungsten center exhibits a diversity of structure that facilitates a range of redox chemistry and reactivity. These enzymes fall into four

Abbreviations: AOR, aldehyde oxidoreductase; CISM, complex iron sulfur molybdoenzymes; EPR, electron paramagnetic resonance spectroscopy; ETR, electron transfer relay; Mo-bisPGD, Mo-bis(pyranopterin guanine dinucleotide); Moco, molybdenum pterin cofactor; Mo-PCD, Mo-pyranopterin cytosine dinucleotide; SUOX, sulfite oxidase enzymes; TMS, transmembrane segments; W-bisPPT, W-bis(pyranopterin); XDH, xanthine dehydrogenase; XOR, xanthine oxidoreductase.

* Corresponding author. Tel.: +1 780 492 2761; fax: +1 780 492 0886.
E-mail addresses: magalon@ifr88.cnrs-mrs.fr (A. Magalon), joel.weiner@ualberta.ca (J.H. Weiner).

0010-8545/$ – see front matter
doi:10.1016/j.ccr.2010.12.031

Keywords:
Bacterial respiration
Dedicated chaperone
Metalloprotein biogenesis
Molybdenum cofactor
Molybdoenzyme
Nitrate reductase

families based on the cofactor sub-type. Family I is an archaeal family which binds a W-bis(pyranopterin) cofactor and a single [4Fe–4S] cluster. Family II binds either a Mo-pyranopterin or Mo-pyranopterin cytosine dinucleotide. Family II molybdoenzymes often form complexes that include subunits that bind FAD as well as [2Fe–2S] clusters. The diverse Family III enzymes (the dimethyl sulfoxide reductase family) bind a Mo-bis(pyranopterin guanine dinucleotide) cofactor, form transient or stable complexes with [Fe–S]-containing electron transfer subunits as well as soluble and membrane anchor cytochromes. Family IV enzymes bind a Mo-pyranopterin cofactor and interact with a membrane-bound cytochrome. Expression of prokaryotic molybdoenzymes is controlled by transport of Mo into the cell, cofactor biosynthesis, transcriptional regulation of apo-protein expression and riboswitch mechanisms. The biosynthesis of prokaryotic molybdoenzymes is an intricate process, requiring the synthesis of various subunits in the cytoplasm, incorporation of the metal and pterin cofactors, subunit complexation, correct subcellular targeting/transport and in many cases anchoring of the complex to the inner membrane. A series of devoted molybdoenzyme maturation proteins are crucial in various stages of enzyme maturation.

1. Scope of the review

Prokaryotic molybdenum (Mo)-containing enzymes play critical roles in metabolism, agriculture, global geochemical cycles, and health [1]. These enzymes primarily catalyze oxo-transfer reactions for the metabolism or catabolism of nitrogen, sulfur and carbon compounds. The majority of such enzymes contain variations of the pterin-molybdenum cofactor (Moco) although an important subset of these are able to bind tungsten (W) as an alternative to molybdenum [2]. Recent advances in the fields of structural biology, cell biology, and bioinformatics have enabled an emerging understanding of the structure and function of these enzymes. This review focuses on the four families of prokaryotic molybdoenzymes. We first summarize the roles of molybdoenzymes in bacterial metabolic diversity emphasizing recent advances of bacterial molybdoenzyme structure, function and expression. We then review the various processes bacterial molybdoenzymes must undergo for formation of an active and correctly located complex and the role of system-specific chaperones. We also identify unanswered questions and future directions for bacterial molybdoenzyme research.

2. Introduction

2.1. Molybdenum and tungsten in prokaryotes

Although only a minor constituent of the Earth's crust, Mo is readily available due to its presence as a trace element in aquatic environments (as molybdate, MoO_4^{2-}). Prokaryotic species that do not require Mo use W (as tungstate, WO_4^{2-}) [3]. The utility of Mo (or W) is based on its incorporation into the organometallic cofactor that serves as a scaffold to bind Mo (or W) and allows the metal to catalytically cycle through the IV, V, and VI oxidation states. Importantly, this enables these enzymes to connect the two electron Moco-catalyzed reaction to an additional active site *via* an electron transfer relay (ETR) able to sequentially transfer single electrons to the distal second site. Examples of this include enzymes that *oxidize* formate and *reduce* quinone and those that *oxidize* quinol and *reduce* nitrate [1,4–6].

2.2. The choice of molybdenum versus tungsten

Why did evolution select Mo and W as the metal component of the pterin cofactor? In oxic aqueous systems, these metals exist in the form of their tetrahedral MoO_4^{2-} or WO_4^{2-} oxyanions, and are therefore easily mobilizable into enzyme systems with the important caveat that they must be distinguished during enzyme maturation to ensure proper redox function and therefore catalysis. The rationale for the existence of both Mo and W-containing enzymes is based on the evolution of life on earth and the impact of this life on its biosphere [1,7]. Prior to approximately 2.3 billion years ago the earth's biosphere was essentially anoxic, high in sulfur, and highly reducing. Mo and W have broadly equivalent natural abundance in the earth's crust at about 1.2 ppm, but sulfides of W are soluble in water whereas those of Mo are not [8]. As a result, W would have been bioavailable in the primordial earth's biosphere whereas Mo would not [9]. Following the evolution of biological water oxidation [10], photosynthetic organisms caused a dramatic increase in ambient redox potential that paralleled the increase in atmospheric oxygen, and this resulted in the appearance and bioavailability of Mo in the form of MoO_4^{2-}. As a consequence, the bioavailability of the two elements were reversed, with Mo being present at a concentration in sea water at 100 times that of W [11]. It is interesting to note that the processes that rendered Mo bioavailable had the opposite effect on iron bioavailability, with increasing oxygen concentrations oxidizing iron(II) to iron(III) oxyhydroxides which are essentially insoluble [12,13].

Both elements are able to assemble into mononuclear molybdoenzymes in an essentially identical manner. This presents a critical biological problem, because redox reactions catalyzed by W typically occur at much lower potentials than those catalyzed by Mo, and the active sites of the enzymes have evolved to modulate the redox properties of their cognate metal ion. Thus, assembly of W in place of Mo in a *bona fide* molybdoenzyme would elicit dramatic changes in catalytic efficacy. This has been demonstrated using W-substituted dimethyl sulfoxide reductase from *Rhodobacter capsulatus* in which the (V/VI) and (IV/V) redox potentials were decreased by −220 and −334 mV, respectively [14]. The W-substituted enzyme is able to catalyze dimethyl sulfoxide reduction (the *forward* reaction), but cannot catalyze dimethylsulfide oxidation (the *backward* reaction) [14]. In *E. coli* trimethylamine-*N*-oxide reductase, substitution with W also results in retention of catalysis in the *forward* direction while considerably perturbing its substrate specificity [15]. In the case of sulfite oxidase, W substitution results in completely inactive enzyme [16]. In the aldehyde:ferredoxin oxidoreductase of *Pyrococcus furiosus*, substitution of Mo for W results in enzyme unable to catalyze aldehyde oxidation [17]. The toxicity of W towards molybdoenzymes and the inferred toxicity of Mo towards tungstoenzymes present cells with a serious problem: toxicity of the antagonist oxyanion *via* incorrect metal insertion. Mo and W have the same atomic radii (1.75 Å and 1.78 Å, respectively), the same electronegativity, the same free energy of solvation (−226.8 kcal mol^{-1} and −230.1 kcal mol^{-1}, respectively) and the same covalent solution radii (2.75 Å and 2.83 Å, respectively). In order to distinguish them, exquisitely discriminating systems have evolved at the levels of metal uptake into bacterial cells [18,19], metal insertion into the cofactor [20–22] and the possible interplay of molybdoenzyme specific chaperones with cofactor incorporation [23–27].

2.3. The structure of the molybdenum cofactor

This review focuses on bacterial enzymes containing the mononuclear molybdenum cofactor (Fig. 1). The cofactor appears in four basic configurations, whose structures have been determined by a combination of rigourous biochemical studies and confirmed by the emergence of a large amount of structural data [28–32]. The cofactor *typically* has a tricyclic pyranopterin structure, with pyrimidine, pyrazine, and pyran rings, respectively labelled *a*, *b*, and *c* in Fig. 1A. The alternative form of the pterin is the bicyclic molybdopterin form, which contains the pyrimidine and pyrazine rings but contains an open pyran ring (see Fig. 1D, distal pterin). Mo and W coordination is *via* two dithiolene sulfurs, which are attached to the pyran ring. Also attached to this ring is a phosphomethyl group, and it is the presence of a terminal phosphate that has led to this form of the cofactor being referred to as a *mononucleotide*. Given the dominance of the pyranopterin structure (tricyclic) over the original molybdopterin (bicyclic) structure developed on the basis of chemical studies [28–30], we propose that it be referred to as Mo-PPT or W-PPT when complexed with Mo or W, respectively. Mo-PPT is the form of the cofactor found in eukaryotes and in essentially all sulfite oxidase enzymes (SUOX) and some xanthine dehydrogenase enzymes (XDH). PPT can be modified by the addition of a nucleotide (typically cytosine or guanine) [33] at the phosphomethyl position to generate a dinucleotide form (Fig. 1C and D). Intriguingly, two PPTs can coordinate a single W atom *via* a pair of dithiolenes (Fig. 1B). This form of the cofactor is the bis-mononucleotide form. The vast majority of bacterial molybdoenzymes contain the molybdo-bis(pyranopterin guanine dinucleotide) (Mo-bisPGD) (Fig. 1D) cofactor or its tungsto derivative (W-bisPGD). A minority of the Mo-bisPGD cofactors contain both a tricyclic pyranopterin ('Proximal pterin' in Fig. 1D) and a bicyclic molybdopterin ('Distal pterin' in Fig. 1D) with a structure similar to that originally proposed for the cofactor by Rajagopalan and co-workers [4,30,34].

Cofactor nomenclature is further complicated in those enzyme subunits that contain both a Mo-bisPGD and an [4Fe–4S] cluster that is at the terminus of an electron transfer relay that can comprise up to five [Fe–S] clusters and two hemes [35]. In the original structure determinations of the Mo-bisPGD containing dimethyl sulfoxide reductases (DorA), the two pterins were arbitrarily referred to as "P" and "Q" [36,37]. When these subunits are structurally aligned to those that also contain an [Fe–S] cluster (e.g. FdhF from *E. coli*) [38], the P-pterin is coincidentally located proximal to the [4Fe–4S] cluster, whereas the Q-pterin is located distal to it. We therefore propose that the proximal pterin be referred to as the P-pterin, and the Q-pterin be referred to as the D-pterin, or distal pterin.

3. The four families of prokaryotic molybdoenzymes

With the exception of the nitrogenase molybdoenzymes (discussed elsewhere in this volume), Mo (or W) in prokaryotes is coordinated by either the mono or a bispyranopterin cofactor buried in the catalytic subunit [35,39–41]. Coordination is supplemented by the sidechain of a cysteine, seleno-cysteine, serine, or aspartate residue and/or by coordination of single oxygen or sulfur atoms in the form of oxo or sulfido groups.

The prokaryotic molybdoenzymes fall into four families based on the type of cofactor bound (see Fig. 2). (I) The archaeal aldehyde oxidoreductase family utilizes a bis-pyranopterin cofactor (W-bisPPT) that typically contains a W atom and lacks a protein-W ligand (Fig. 1B) [42,43]. (II) The xanthine dehydrogenase family, exemplified by *Rhodobacter capsulatus* xanthine dehydrogenase (*Rh*XDH) [44] contains a Mo atom coordinated by a single pterin (Mo-PPT as seen in Fig. 1A or Mo-PCD in Fig. 1C), lacks a protein-Mo ligand, but contains an additional sulfur in the coordination sphere (an important distinction between Family I and Family II molybdoenzymes). (III) The prokaryotic dimethyl sulfoxide reductase family is expemplified by *E. coli* nitrate reductase and contains a Mo-bisPGD cofactor (Fig. 1D) with a cysteine, seleno-cysteine, serine, or aspartate protein Mo-ligand [4,35,37,45,46]. (IV) The sulfite oxidase family contains a single pyranopterin cofactor (Fig. 1A) and a conserved cysteine as the protein-Mo ligand and is exemplified by the *E. coli* YedY protein [41,47–49].

3.1. Family I molybdoenzymes

The archaeal aldehyde oxidoreductase family (Fig. 2A). These enzymes catalyze the oxidation of an aldehyde to an acid, with electrons being transferred to a soluble ferredoxin (similar reactions are also catalyzed by a subset of the Family II enzymes, see Section 3.2 below). This family is distinguished by the presence of a W-bisPPT cofactor and the best-characterized examples are found in the hyperthermophilic archaeon *P. furiosus*, with examples including formaldehyde:ferredoxin oxidoreductase (FOR) [50], glyceraldehyde-3-phosphate:ferredoxin oxidoreductase (GAPOR) [51], aldehyde oxidoreductase (AOR) [45], as well as the YdhV subunit of the *E. coli* YdhYVXU operon [52]. It is notable that the first structure determined of a mononuclear Mo/W enzyme was that of the *P. furiosus* AOR [42,53]. It is a dimer composed of two 605 residue subunits. Each subunit binds a W-bisPPT cofactor and a [4Fe–4S] cluster. The structure revealed several novel features which are applicable to many other Mo-containing enzymes including the finding that the W was coordinated by the dithiolenes of two anti-parallel pyranopterins.

3.2. Family II molybdoenzymes

The xanthine dehydrogenase and aldehyde oxidase family (Fig. 2A). The enzymes of this family are involved in two-electron transfer hydroxylation and oxo-transfer reactions with water as the source of oxygen [54]. Members of this family include xanthine dehydrogenases (XDH) involved in purine catabolism and aldehyde oxidases which oxidize numerous aromatic and non-aromatic heterocycles and aldehydes to yield their respective carboxylic acids. The Mo active site of these enzymes is characterized by a cyanolysable sulfur ligand, typically a sulfido group. Mo sulfuration, and thus enzyme activation, occurs either concurrently or after Mo-PPT/PCD insertion into the enzyme (see Section 7.2) [39,55,56]. Members of this family contain one to three subunits with a similar modularity to that of the Family III enzymes discussed below. While the eukaryotic xanthine oxidoreductase (XOR) exists as a dimer of monomers, each of which contains a flavin adenine dinucleotide cofactor (FAD), two non-identical [2Fe–2S] clusters, and a Mo-PPT cofactor, prokaryotic XDH's and AOR's are more complicated in structure. For example, *Pseudomonas putida 86* Quinoline 2-oxidoreductase (QorMLS) contains three separate subunits for each type of cofactor: i.e. an FAD binding subunit (QorM), Mo-PCD binding subunit (QorL), and QorS which binds two non-identical [2Fe–2S] clusters [57,58]. Alternatively, *Rhodobacter capsulatus* XDH is a dimer of dimers combining a fusion of the FAD and [2Fe–2S] subunits into one. Electron transfer proceeds from Mo → [Fe–S] I → [Fe–S] II → FAD and finally to NAD^+. In a different variation *Desulfovibrio gigas* aldehyde oxidase (*Dg*MOP) does not contain FAD and electrons are transferred through a complex of several subunits with 11 redox center to form hydrogen [44,54,59–61].

3.2.1. Xanthine dehydrogenase from Rhodobacter capsulatus

*Rh*XDH is a cytoplasmic enzyme complex that catalyzes the oxidation of hypoxanthine to xanthine and finally to uric acid,

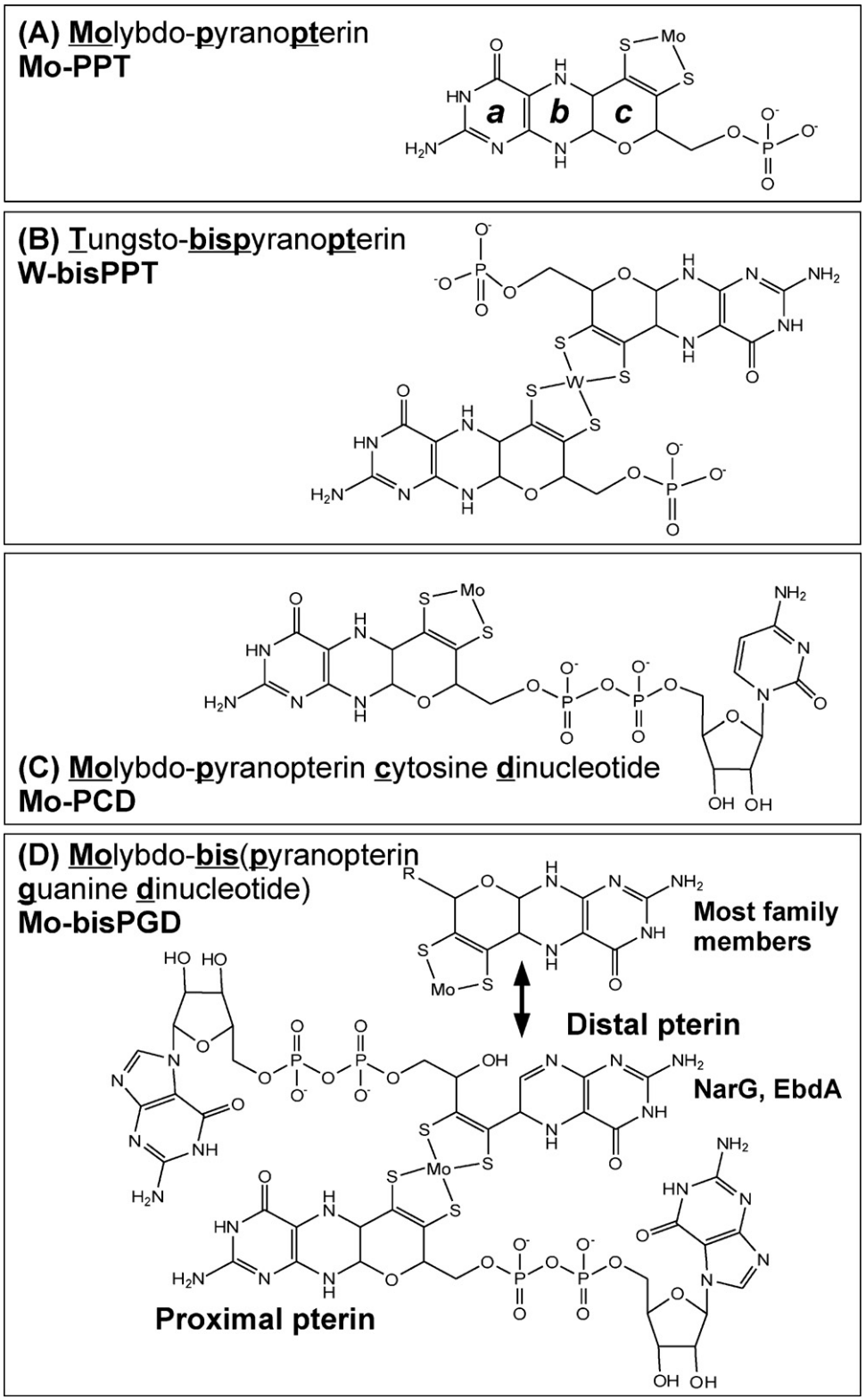

Fig. 1. Structures and nomenclature of the mononuclear molybdenum cofactor. (A) The molybdo-pyranopterin cofactor (Mo-PPT) found in eukaryotic molybdoenzymes, bacterial xanthine dehydrogenases (XDH) and sulfite oxidases (SUOX) [41,162]. The substituent rings of the pterin are (a) pyrimidine, (b) pyrazine, and (c) pyran. (B) The tungsto-bis(pyranopterin) cofactor-(W-bisPPT) found in the archaeal aldehyde oxidoreductases [42]. This form of the cofactor can also be referred to as a bis-mononucleotide form of the mononuclear tungsten cofactor. (C) The molybdo-(pyranopterin cytosine dinucleotide) cofactor (Mo-PCD) found in most bacterial xanthine dehydrogenases [54,56,170,235,236]. (D) The molybdo-bis(pyranopterin guanine dinucleotide) cofactor (Mo-bisPGD) found in the majority of bacterial molybdoenzymes that can also exist in a W-bisPGD form. In two examples, the *E. coli* respiratory nitrate reductase (NarGHI) [4] and the ethylbenzene dehydrogenase (EbdABC) from Aromatoleum aromaticum [34], one of the pterins has the bicyclic molybdopterin structure predicted from the chemical studies of Rajagopalan and coworkers [28,29,31]. Mo-bisPGD can also be referred to as a bis-dinucleotide form of the mononuclear molybdenum cofactor.

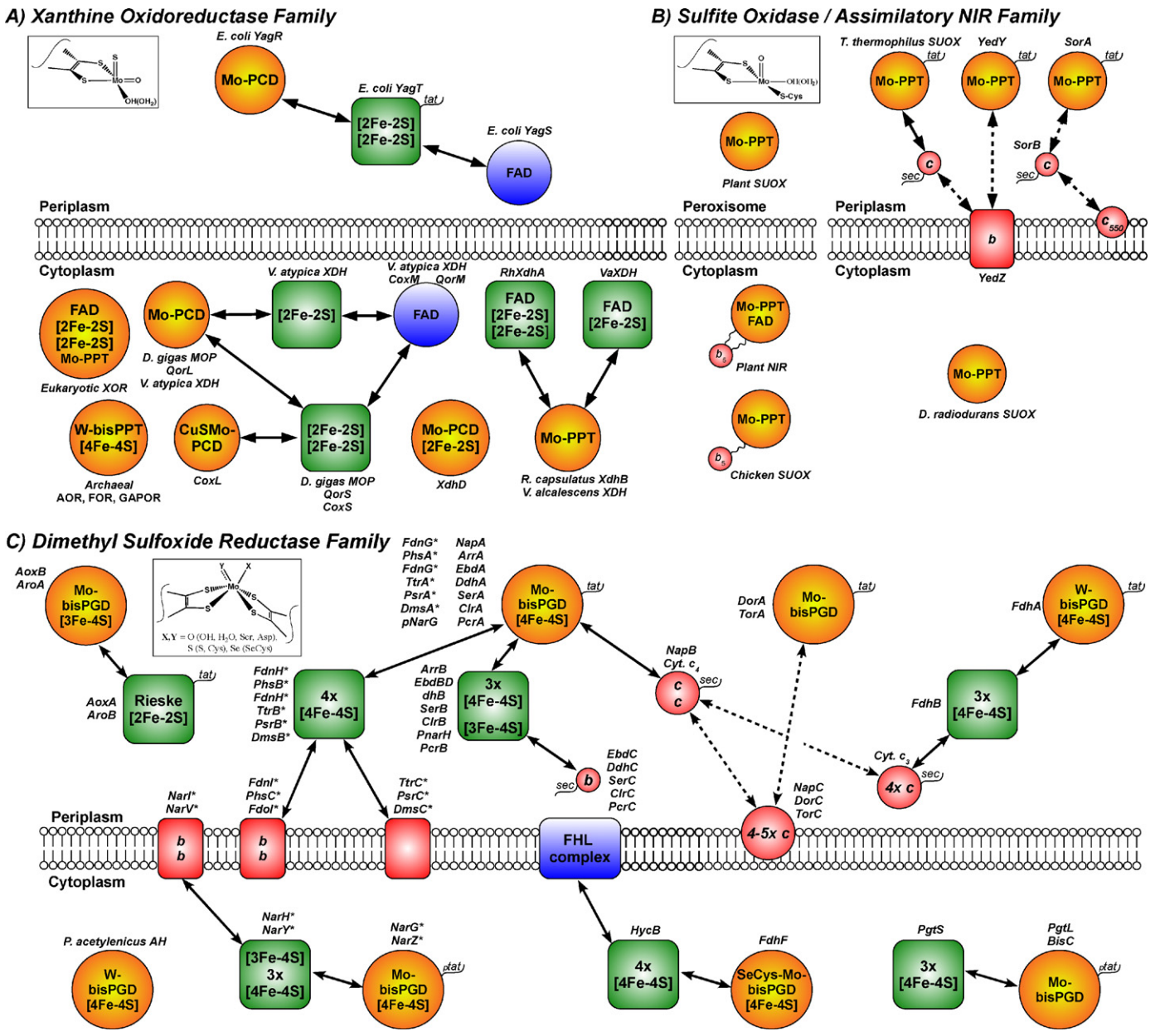

Fig. 2. Molybdoenzyme subunit diversity. Discussion of the entire plethora of bacterial molybdoenzymes is beyond the scope of this review. Bayman et al. [237] described the concept of the redox enzyme subunit toolkit, in which a variety of subunit/domain modules come together to generate specific metabolic functionalities that contribute to metabolic diversity. Subunits can be "mixed and matched" to generate systems interfacing with membrane-intrinsic quinone pools, cytochromes c, flavoproteins, and ferredoxins. Represented by the orange circles are the Mo/W-pterin-containing enzymatic subunits, green boxes represent electron-transfer subunits, blue circles are flavoproteins, red circles and squares indicate cytochromes; the blue square is the FHL complex. Subunits that contain a Tat leader (*tat*), pseudo-Tat leader (*ptat*), or Sec leader (*sec*) are indicated by a correspondingly labelled squiggle coming off the respective subunit [35,41,196,238]. Interactions between various subunits are of two types: transient interactions (dashed-line arrows) such as between YedY and YedZ, or strong interactions (solid-line arrows) as in the heterotrimer of NarGHI. (A) The archaeal/bacterial/eukaryotic xanthine dehydrogenase (XDH) and aldehyde oxidoreductase (AOR) families. Archaeal refers specifically to *P. furiosus* (FAD – flavin adenine dinucleotide; AOR – aldehyde:ferredoxin oxidoreductase; FOR – formaldehyde:ferredoxin oxidoreductase; GAPOR – glyceraldehyde-3-phosphate:ferredoxin oxidoreductase; MOP – *Desulfovibrio gigas* AOR) [42,53,54,56–60,235,239–244]. (B) The members of the sufite oxidase (SUOX) and assimilatory nitrate reductase (NIR) family [41,48,49,123,128,131,245–250]. (C) The members of the dimethyl sulfoxide reductase family. Archetypal members of the CISM group are indicated with an asterisk. (FHL – Formate Hydrogen Lyase complex; SeCys – Selenocysteine; AH – Acetylene Hydratase; cyt – cytochrome) [4,9,34,35,37,66,74,78,82,84–86,166,171,251–255]. The figure does not convey multimerization of enzyme complexes: NarGHI is actually a dimer of trimers, Plant NIR is a homodimer, *P. furiosus* AOR is a homotetramer, etc. For further information on the enzyme systems, refer to references or search using the given genotypes. *E. coli*, *Escherichia coli*; *D. gigas*, *Desulfovibrio gigas*; *V. atypica*, *Veillonella atypica*; *R. capsulatus*, *Rhodobacter capsulatus*; *V. alcalescens*, *Veillonella alcalescens*; *T. thermophilus*, *Thermus thermophilus*; *D. radiodurans*, *Deinococcus radiodurans*; *P. acetylenicus*, *Pelobacter acetylenicus*.

using NAD^+ as an electron acceptor. The *Rh*XDH has a sequence, subunit organization, and cofactor content more similar to eukaryotic xanthine oxidoreductase than to other bacterial XDHs [59,60]. However, unlike eukaryotic XOR it lacks the critical cysteine residues that allow XOR to interconvert between the oxidase and dehydrogenase forms and thus *Rh*XDH is limited to NAD^+ as an electron acceptor [44,59,60,62]. *Rh*XDH is composed of two subunits, encoded by the genes *xdhA* and *xdhB*, which together form a butterfly shaped dimer ($\alpha_2\beta_2$) [44]. Sequence analysis shows homology between XdhAB with the *E. coli* periplasmic XDH YagTSR and *Dg*MOP, where sequence variability in the enzymatic subunits may be due to the different Moco bound: Mo-PPT in the case of *Rh*XDH, and Mo-PCD in the case of the other two [54,56,59].

*Rh*XdhA is 50 kDa and consists of two domains: the N-terminal domain binds the two [2Fe–2S] clusters, while the C-terminal domain binds an FAD. The two domains are joined by a 31 residue peptide linker which is homologous to the linker region in eukaryotic XOR. In eukaryotes this linker facilitates interconversion between the dehydrogenase and oxidase forms, but *Rh*XdhA lacks the necessary cysteines for this to occur. The N-terminal [2Fe–2S] domain contains a ferredoxin-type four-helix bundle with twofold symmetry that binds a [2Fe–2S] cluster at the apex, which inserts into *Rh*XdhB and seals the Moco from the solvent. The second cluster, proximal to FAD, lies 12.4 Å from the first cluster and is coordinated by a plant and cyanobacterial-like ferredoxin fold. Since all redox cofactors are within 14 Å of each other a "through-space" electron transfer mechanism has been proposed [63]. The C-terminal FAD domain is only 22% identical in sequence to bovine XDH however it is structurally very similar.

The Moco subunit, *Rh*XdhB, is 85 kDa and can be subdivided into two domains: Mo1 and Mo2, with the Moco being situated between the two domains and close to the XdhA–XdhB interface. The Moco itself is of the Mo-PPT variety, as are all eukaryotic XORs. Mo1 and Mo2 can each be subdivided into two subdomains, each having extensive β-sheet structure with one or two interacting α-helices. The overall fold of *Rh*XdhB is homologous to bovine milk XDH, *Dg*MOP, and *Oligotropha carboxidovorans* CO dehydrogenase (CoxMSL). The Mo-PPT is bound tightly to the enzyme *via* several highly conserved side-chain and main-chain interactions. Mo itself is coordinated by the two dithiolene sulfurs of PPT, an oxo and sulfido group, and water [44,60].

3.3. Family III molybdoenzymes: the dimethyl sulfoxide reductase family (Fig. 2C)

This family includes the periplasmic dimethyl sulfoxide reductase of *Rhodobacter sphaeroides* and *Rhodobacter capsulatus* that were the first members of the family to be structurally characterized [36,37]. It is widespread in prokaryotes and has been extensively reviewed [35,64]. These enzymes can be simple soluble proteins with only a Mo-bisPGD cofactor such as trimethylamine-*N*-oxide reductase (TorA) (see Section 3.3.1) [65], dimethyl sulfoxide reductase (DorA) [36], and biotin sulfoxide reductase (BisC) [66].

At the next level of complexity, the Mo-bisPGD-containing subunit can pair up with a heme-containing electron-transfer subunit as in the periplasmic NapAB found in many eubacteria (see Section 3.3.2) [67]. At the most complex level these molybdo-subunits can be part of multi-subunit membrane-bound proteins of which a large number have been characterized at the structural, functional and biophysical level (see Section 3.3.3).

3.3.1. Family III enzymes with only a Mo-bisPGD cofactor

These enzymes are soluble and coordinate Mo-bisPGD as the only cofactor. They can be located in either the cytoplasmic or periplasmic compartments of diderm prokaryotes. Periplasmic localization is determined by the presence of an N-terminal twin arginine translocation (Tat) leader sequence [68–73]. Many members of this group have been extensively studied including the periplasmic dimethyl sulfoxide reductase (DorA) that reduces dimethyl sulfoxide to dimethylsulfide [74], the periplasmic trimethylamine-*N*-oxide reductase (TorA) [65] that reduces trimethylamine-*N*-oxide to trimethylamine and the cytoplasmic biotin sulfoxide reductase (BisC) [66] that converts biotin sulfoxide to biotin. In the case of the periplasmically localized TorA and DorA, interaction with the Q-pool is transiently through a membrane intrinsic penta-heme cytochrome c: TorC and DorC [74].

Many of these enzymes have been crystallized and extensively examined at the structural and biophysical levels. Following the initial reports on the 2.2 Å and 1.88 Å resolution structures of dimethyl sulfoxide reductases of *R. sphaeroides* [36] and *R. capsulatus* [37] various Mo co-ordination environments in the oxidized Mo(VI) state were proposed. However, very high resolution (1.3 Å) crystallographic data revealed that the previously reported structures represented an average of several conformations [75]. Similar conclusions were reached in a recent X-ray absorption spectroscopy study of trimethylamine-*N*-oxide reductase [76]. Heterogeneity at the active site seems to be a feature of many molybdoenzymes of the dimethyl sulfoxide reductase family, which complicates spectroscopic and structural investigations [77]. DorA, which is a typical example of the family, is comprised of 780 residues encompassing four conserved domains (see Fig. 3A) [37,46]. Domains I and II lie on one side of a cup-shaped protein that co-ordinates the Mo-bisPGD. Domain III forms the opposite side of the cup with the Mo atom at the bottom of the cup which is open to the external environment. Domain IV lies beneath the Mo atom and closes the channel. Domains II and III comprise the nucleotide binding domain of pterins D and P, respectively. The pterin part is bound by domain IV. The PGD bound to domain II is called the P-PGD and the PGD bound to domain III is the D-PGD [36]. The Mo-bisPGD is comprised of two antiparallel pyranopterins with a twofold axis of symmetry through the Mo (see Fig. 1D). The Mo atom is co-ordinated by four dithiolene sulfurs, the sidechain of an amino acid (serine, cysteine, seleno-cysteine) and an additional oxo group. The protein makes over 45 contacts with the cofactor. Detailed information on the geometry and ligation of the Mo is discussed elsewhere in this volume.

The trimethylamine-*N*-oxide reductase of *E. coli* (TorA) has been extensively studied and provides insights into the maturation of molybdoenzymes as discussed below (see Section 7.1.2). TorA binds a Mo-bisPGD and communicates with a c-type pentaheme periplasmic protein (TorC) that is held to the membrane by an N-terminal anchor [65]. TorA primarily reduces trimethylamine-*N*-oxide and 4-methylmorpholine-*N*-oxide and does not reduce dimethyl sulfoxide. The structure of *Shewanella massilia* TorA has been determined [78]. The arrangement of the polypeptide around the Mo-bisPGD is typical for this family as described above. The Mo is buried within the protein and substrates reach the active site *via* a wide funnel as in the DorA protein. An interesting aspect of the *Ec*TorA is that W could replace the transition metal Mo [15] and the modified enzyme used both trimethylamine-*N*-oxide and dimethyl sulfoxide. Attempts to incorporate W in other *E. coli* molybdoenzymes results in non-functional protein entirely devoid of Mo-bisPGD [79,80].

3.3.2. Family III enzymes with Mo-bisPGD and an [Fe–S] cluster

A major difference between this group and the enzymes described above is that a [4Fe–4S] cluster is ligated by domain I in close proximity to the Mo-bisPGD at a motif sequence Cys–X_2–Cys–X_3–Cys–$X_{24\text{-}26}$–Cys [81]. This motif is found in most members of the dimethyl sulfoxide reductase family with some variations as in NarG/EbdA/SerA/DdhA where the first cysteine is replaced by a histidine (see Section 3.3.3) or in AroA which binds a [3Fe–4S] cluster with a Cys–X_2–Cys–X_3–Cys motif [82]. The [4Fe–4S] cluster and Mo-bisPGD are about 12 Å apart. This group can be further sub-divided into those proteins that bind a heme-containing subunit and those that bind an [Fe–S]-containing electron transfer subunit.

These enzymes are distinguished from the more complicated complex iron-sulfur molybdoenzymes (CISM), described in Section 3.3.3, by the arbitrary limit of no more than two subunits and/or the lack of a membrane anchor subunit. The catalytic subunit containing the cofactor and [Fe–S] cluster can be paired with a diheme cytochrome c in the case of NapAB, or [2Fe–2S] cluster-containing

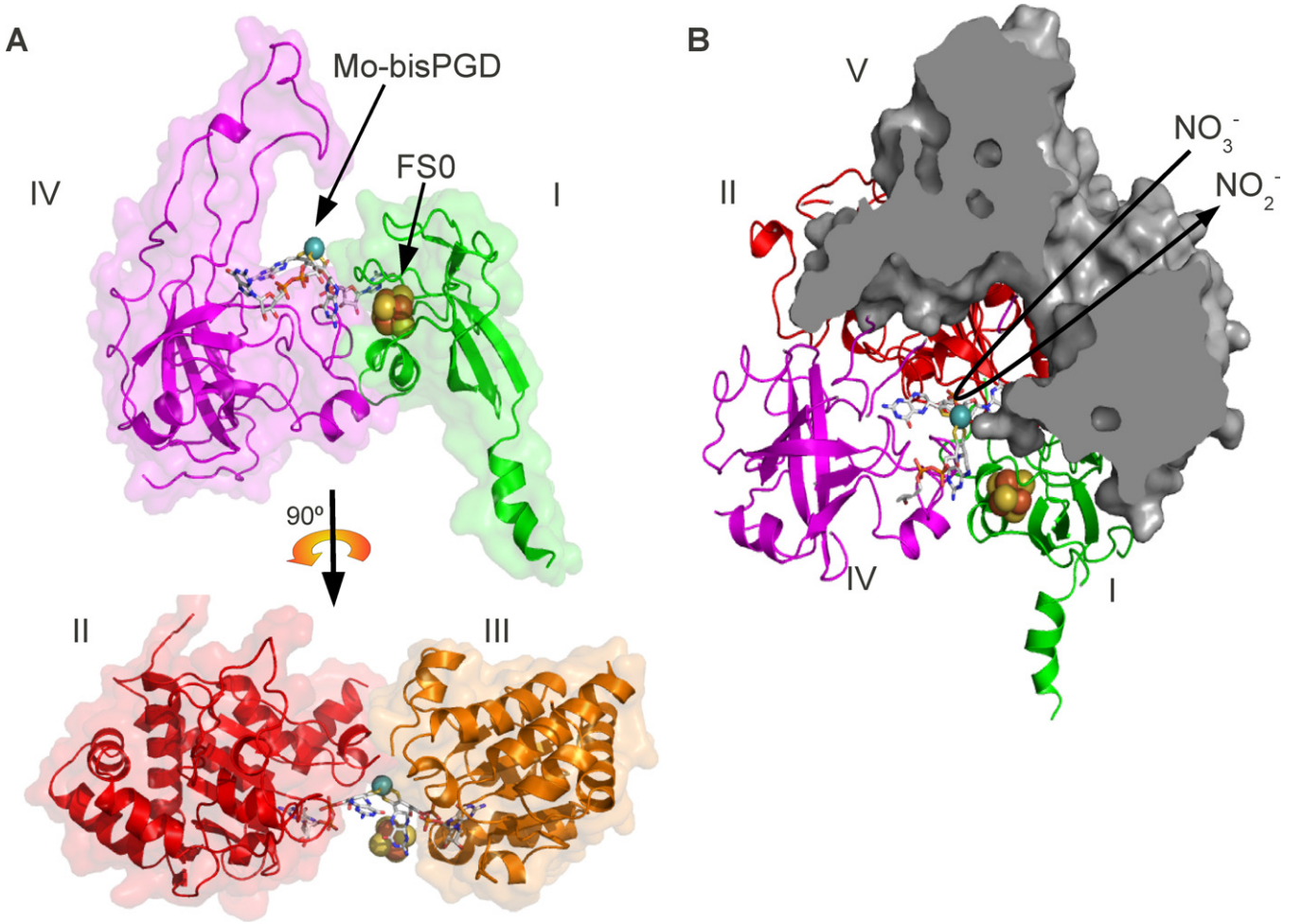

Fig. 3. Domain structure of the catalytic subunits of Family III molybdoenzymes. (A) The four conserved "core" domains (I–IV) of the DMSO Reductase family of molybdoenzymes is exemplified by the structure of NarG (PDB ID code 1q16) [46]. The upper pane shows domain I, which coordinates FS0, and domain IV, which binds the pterin portion of Mo-bisPGD. A 90° counter-clockwise rotation along the *y*-axis provides a view of domains II and III, which bind the guanine moieties of Mo-bisPGD. (B) The additional domain V of NarG provides a narrow and elongated substrate channel for nitrate/nitrite access.

subunit in the case of arsenite oxidase [82]. More complex CISM-like members of this group are ethylbenzene dehydrogenase (EbdABC), chlorate reductase (ClrABC), selenate reductase (SerABC), and dimethyl sulfide dehydrogenase (DdhABC), perchlorate reductase (PcrABC) which all contain a catalytic subunit that coordinates a Mo-bisPGD and a [4Fe–4S] cluster, a electron transfer subunit with three [4Fe–4S] clusters and one [3Fe–4S] cluster, and most importantly a soluble cytochrome *b* subunit [34,83–86].

The periplasmic nitrate reductase NapAB is typical of dimeric CISM-like molybdoenzymes. NapAB is widely distributed in bacteria where it is necessary for nitrate scavenging by pathogenic species [87]. It is normally found as a dimer (NapAB) (an exception is the *Desulfovibrio desulfuricans* NapA which is monomeric and soluble in the periplasm [88]. NapA (~91 kDa), the catalytic subunit, reduces nitrate to nitrite. The electrons required for reduction are transferred from the diheme cytochrome c, NapB (17 kDa) [89]. The NapAB dimer ultimately derives its electrons from ubiquinol or menaquinol through NapC, a membrane-bound globular tetraheme cytochrome c with which NapAB interacts transiently [90].

The genomic organization of the *nap* operon is complex and there is evidence that *napABCD* genes are necessary but not *napFGH* for periplasmic nitrate reduction [87,91,92] but this varies among different bacterial species with apparent species dependent assembly pathways (see below). In the oxidized state of NapA, the Mo is hexacoordinated in which the Mo is coordinated by four dithiolene sulfurs from PGD, a cysteine from the protein, and a 6th ligand which was originally believed to be an oxo, until the interpretation of the 1.99 Å-resolution X-ray data of the "as-prepared" enzyme from *D. desulfuricans* suggested that it is a sulfur [93]. This would have significant implications regarding the catalytic mechanism if it were established that this corresponds to an active state. Recent electrochemical studies have revealed the existence in *R. sphaeroides* NapAB of several states that stand apart from the reaction pathway and may have been mistaken for catalytic intermediates; this has been discussed in relation with the heterogeneity of the Mo(V) EPR signal of all enzymes of the dimethyl sulfoxide reductase family [77,94].

3.3.3. The complex iron-sulfur molybdoenzyme (CISM) group

Considerably more complex members of Family III are the membrane-bound heterotrimeric proteins, where in Fig. 2C the subunits belonging to this group are indicated by an asterisk [35]. These enzymes are composed of three distinct subunits: a large catalytic subunit containing the active site, the Mo-bisPGD and a [4Fe–4S] cluster; an electron transfer subunit coordinating 4 [Fe–S] clusters; and an integral membrane anchor subunit that may coordinate *b*-type hemes and provides the quinol oxidation/reduction site. These enzymes differ from the other two Family III molybdoenzyme groups (NapAB, TorA, DorA, etc.) in that their interaction

with the membrane intrinsic subunit is a stable interaction that forms a membrane-bound complex, whereas with the interaction of NapAB, TorA, DorA with their membrane-bound counterparts is transient (NapABC, TorAC, DorAC). This group includes the formate dehydrogenase-N (FdnGHI) [6], dimethyl sulfoxide reductase (DmsABC) [95] and nitrate reductase (NarGHI) [96] from *E. coli*. The architecture of this family has been verified by the high-resolution structure of *Ec*NarGHI [4,46] as well as the structures of *Ec*FdnGHI [6] and *Thermus thermophilus* polysulfide reductase (PsrABC) [97]. These structures, when combined with a wealth of available biochemical and biophysical data clearly put us on a path to an atomic resolution understanding of this group of molybdoenzymes.

The membrane anchor subunits are the most variable of the subunits in the CISM group. They can vary from 4 TMS in FdnI [6], 5 TMS in NarI [4] to 8 TMS in DmsC [98] and PsrC [97]. They may (NarI, FdnI) or may not (DmsC, PsrC) coordinate *b*-type hemes. What they all have in common is a quinone binding site for the oxidation or reduction of menaquinone and/or ubiquinone and an anchoring function for the extrinsic catalytic and electron transfer subunits. For example, FdnI, the anchor of the FdnGHI complex has 4 TMS in which the two hemes are coordinated by 2 histidine residues from one helix (TMS 4), with the other two coming from TMS 1 and 2. Thus, in FdnI the proximal heme b_P (proximal to the membrane-extrinsic dimer) is coordinated by histidine residues from TMS 2 and 4, and distal heme b_D (distal to the membrane-extrinsic dimer) is coordinated by histidine residues from TMS 1 and 4 [6]. In comparison with NarI, there is an unfortunate lack of spectroscopic and potentiometric data on the hemes of FdnI. Another variation is represented by the PsrC/DmsC anchors of *Thermus thermophilus* polysulfide reductase (PsrABC) and *E. coli* dimethyl sulfoxide reductase (DmsABC), respectively. These anchors are organized in eight TMS and lack heme [95]. The structure of PsrABC has recently been determined [97] providing new insight into the organization of these eight TMS subunits [97]. Co-crystallization of PsrABC with quinones shows that the quinone binding site is close to the periplasmic side of the membrane near iron sulfur cluster FS4, in PsrB. A strictly conserved arginine found in DmsC, PsrC, TtrC, and NrfD may play a role in stabilizing the helices of the subunit, similar to a conserved histidine in FdnI, but this arginine is too far from the Q-site to be involved in quinone binding (10 Å) [6,97,99]. Interestingly, this arginine may also serve as part of a proton translocating pump, since PsrABC has been shown to translocate a proton for every two electrons transferred and mutation of this conserved residue in *W. succinogenes* PsrC resulted in an inactive enzyme [97,99]. In DmsC the quinone site must also be close to FS4 and although the arginine is conserved, DmsABC is not electrogenic and does not pump protons [100].

One notable aspect of the CISM group is the orientation of the catalytic and electron transfer subunits with respect to the cytoplasmic membrane. CISM enzymes oriented to the external, periplasmic face are addressed to this location *via* the twin arginine translocon (Tat) by the signal sequence at the N-terminus of the catalytic subunit (see below) [35,69]. In enzymes that lack a Tat signal peptide, the catalytic and electron transfer subunits are oriented to the inner face of the cytoplasmic membrane. One consequence of this membrane topology is that a complete respiratory chain can comprise two members of the CISM group with their catalytic dimers having opposite orientations with respect to the cytoplasmic membrane. The membrane-soluble quinone pool allows communication between the two enzymes. The process of proton translocation (contributing to the generation of the protonmotive force) is achieved by distributing the H^+-releasing and H^+-consuming reactions across the energy conserving membrane. This is defined as a "redox loop mechanism" for energy conservation as proposed by Peter Mitchell in his Chemiosmotic Theory (Section 6) and exemplified by the formate dehydrogenase-N: nitrate reductase respiratory chain [101,102].

3.3.3.1. Escherichia coli nitrate reductase A: an archetypal CISM (Fig. 4). For brevity we discuss only the quinol:nitrate oxidoreductase of the anaerobic respiratory chain, referred to as the nitrate reductase A (NarGHI), an archetypal member of the CISM group and one of the best characterized complex molybdoenzymes at the structural, biochemical and biophysical levels. NarGHI consists of: (i) a catalytic subunit (NarG), that contains a Mo-bisPGD and a [4Fe–4S] cluster with unique properties (FS0); (ii) an electron transfer subunit (NarH) that contains four [Fe–S] clusters (FS1 to FS4); and (iii) a membrane anchor subunit (NarI) that provides a site of quinol oxidation, as well as anchoring of the catalytic and the electron transfer subunit subunits to the cytoplasmic membrane. NarI contains two *b*-type hemes. Overall the polypeptides form a scaffold to coordinate the electron transfer relay (ETR) that connects the membrane buried quinol oxidation site, in close proximity to one of the hemes, to the nitrate reduction site at the Mo-bisPGD (Fig. 4). The redox interconversion of nitrate to nitrite occurs at the Mo-bisPGD, which is maintained in redox equilibrium with the lipid-soluble quinone pool *via* the electron-transfer relay comprising FS0-FS4 and the hemes of the membrane anchor subunit. Quinone redox chemistry typically occurs at a quinone binding site that is distal to the hemes of the membrane anchor subunit, or at the interface between the four cluster protein and the membrane subunit in the CISMs that do not contain heme (e.g. DmsABC, PsrABC). In the case of NarGHI, the ETR extends over a distance of approximately 98 Å with inter-center distances (edge to edge) between redox components of 5.4–11.2 Å [4].

The catalytic subunit (*NarG*). NarG is 1244 residues in length (139 kDa) and is considerably larger than the majority of dimethyl sulfoxide reductase family catalytic subunits which are about 800 residues. NarG is composed of four conserved domains (Fig. 3A) grouped around the Mo-bisPGD catalytic center, plus a fifth domain (V) that provides a narrow substrate binding funnel leading to the Mo active site (Fig. 3B) [4,46]. In most structurally characterized molybdoenzymes, the Mo coordination sphere comprises the four dithiolene sulfurs of the cofactor, one or two oxo groups, and a cysteine, seleno-cysteine, or serine as protein-Mo ligand. However, in NarG, in addition to the four dithiolene sulfurs from the two pterins, the Mo atom is coordinated by one or both carboxylate oxygens from an aspartate (NarG-Asp222) [4,46]. The two antiparallel pterins also have some unusual properties. In NarG the distal pterin has a bicyclic structure with an open pyran ring (see Fig. 1D) which is probably stabilized by the side chains of Ser791 and His1163 [103]. Whereas the proximal pterin is a typical tricyclic pterin. The Mo(IV → V) and Mo(V → VI) transitions have been determined by redox potentiometry to be E_m = +95 mV and E_m = +190 mV, respectively and enabling stabilization of a Mo(V) species detectable by EPR spectroscopy [104].

NarG coordinates an essential [4Fe–4S] cluster (FS0) in close proximity to the proximal pterin. FS0 is coordinated by 3 cysteines (Cys53, Cys57, Cys92) and a histidine (His49) located near the N-terminus [105]. This coordination is similar to that observed for one of the [4Fe–4S] clusters of the bacterial hydrogenases, such as the [Ni–Fe] hydrogenase from *Desulfovibrio gigas* [106], and the Fe–Mo hydrogenase from *Clostridium pasteurianus* [107]. The NarG [4Fe–4S] cluster has a $S = 3/2$ ground state [105] effectively moving the visible features of its EPR spectrum to a higher *g*-value near $g = 5.0$. Redox potentiometry suggests the cluster has an $E_m = -55$ mV appropriate for participating in the electron transfer relay. However detailed spin quantitation of EPR signals generated by the $S = 3/2$ species revealed that the $g = 5.0$ signals are substoichiometric, suggesting that the FS0 center is also present in another ground state, most likely $S = 1/2$ [108,109]. Mutation of His49 to

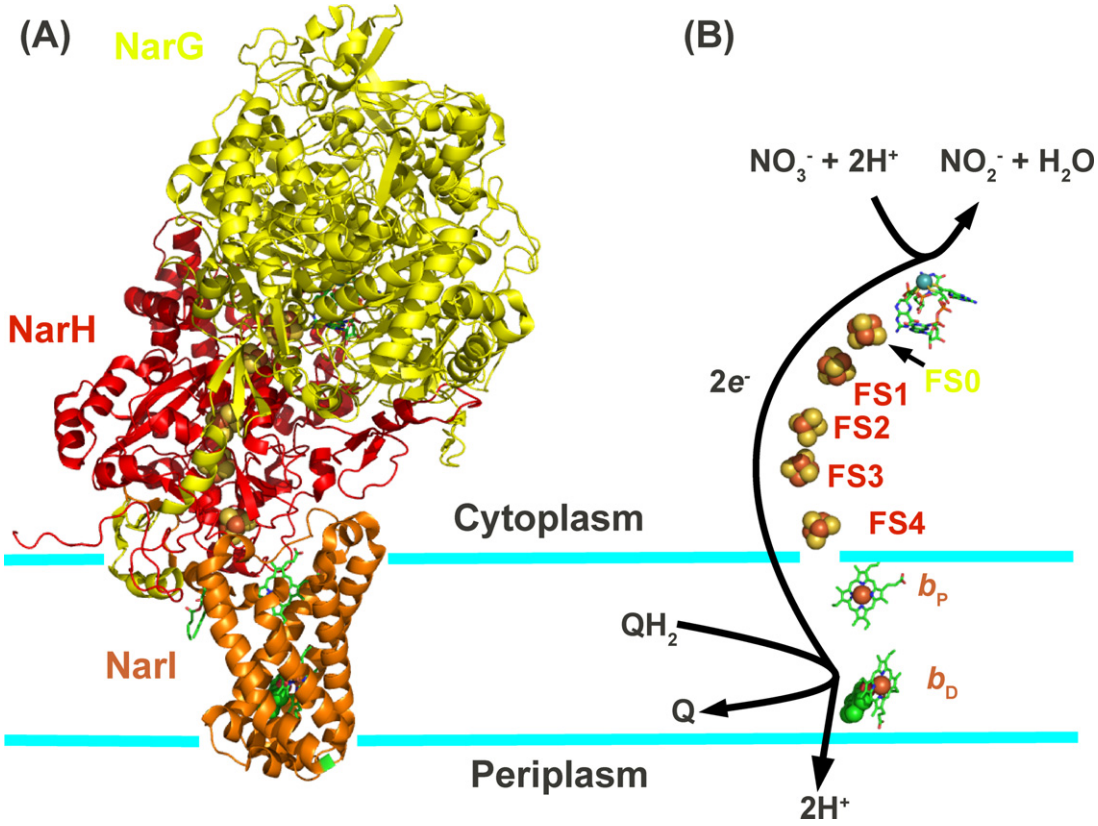

Fig. 4. *E. coli* nitrate reductase A (NarGHI) as an archetypal CISM. (A) The three subunits of NarGHI are shown in yellow (NarG), red (NarH), and orange (NarI). The enzyme is embedded in the cytoplasmic membrane with the NarGH subunits oriented towards the cytoplasmic compartment [4]. (B) The NarGHI electron transport relay comprises two hemes, five [Fe–S] clusters, and a Mo-bisPGD cofactor. It spans ~100 Å from a quinol binding site in NarI [5].

serine or cysteine removes the $g = 5.0$ EPR signal and eliminates catalytic activity [108,110]. X-ray crystallography indicates that NarGHI assembles on the membrane in both mutants and is structurally superimposable on the wild-type structure [110]. In the cysteine variant FS0 and Mo-bisPGD assemble. However, in the serine mutation FS0 and bisPGD are absent with only two guanosine diphosphate molecules occupying the PGD site. The FS0 cluster communicates with Mo-bisPGD *via* Arg94 which is optimally situated for electron transfer. Mutation of this residue to serine causes a dramatic change in the FS0 EPR spectrum and a negative shift in the E_m to −170 mV [110].

The electron transfer subunit (*NarH*). The electron transfer subunits of the CISM group form the scaffold for a series of stepping stones coordinating four [Fe–S] clusters (FS1–FS4) that are crucial for electron transfer relay from the quinone binding site to the Mo-bisPGD. In NarH, FS1 to FS3 are [4Fe–4S] clusters and FS4 is a [3Fe–4S] cluster whereas in most other CISM group members all four clusters are [4Fe–4S]. NarH provides the molecular scaffold to place each cluster in the correct juxtaposition for efficient electron transfer well within the 14 Å edge to edge limit for electron transfer [111].

NarH comprises two domains (A and B) which each coordinate a higher potential and a lower potential cluster [112]. These clusters have midpoint potentials (E_m values) of +130 mV (FS1), −420 mV (FS2), −55 mV (FS3), and +180 mV (FS4) [96]. The clusters are coordinated by four ferredoxin-like cysteine groups (Groups I–IV) (Fig. 5) with a consensus sequence of ($C_ax_2C_Bx_{2-11}C_Cx_3C_DP$) [113]. The protein environment also sets the redox potential of each cluster. Two additional domains of NarH comprise inserts that completely shield the core structure from the aqueous milieu. These domains are missing in other CISM electron transfer subunits. In the earlier literature there was controversy about the role of the very low potential FS2 (−420 mV). FS2 was proposed to serve a structural role as its potential was deemed to be too low and unlikely to participate in direct electron transfer. However the X-ray structure of NarGHI clearly showed that FS2 was an integral member of the electron transfer relay. The low potential can be a barrier to electron flow and may serve to coordinate the rate of electron transfer with the rate of catalysis. Importantly other well-characterized prokaryotic redox enzymes including dimethyl sulfoxide reductase, succinate dehydrogenase and fumarate reductase have a very low potential cluster in the electron transfer chain suggesting that this is a common feature of electron transfer relays [95,114,115]. More work will be required to unequivocally understand the role of FS2.

NarH evolved to coordinate [Fe–S] clusters covering a 600 mV range in E_m values. One approach to understanding the role of potential in overall catalysis has been to apply site directed mutagenesis. For example mutation of NarH Cys26 to alanine results in conversion of FS2 to a [3Fe–4S] cluster [5], raises the E_m by approximately 600 mV (Parkin et al., unpublished) and significantly affects the quinol oxidase activity [113]. One hypothesis that may explain this range is that the hydrogen bonding environment surrounding the clusters is crucial in defining their E_m values.

The membrane anchor and quinol oxidizing subunit (*NarI*). NarI is comprised of 225 residues organized in five transmembrane segments (TMS) to coordinate two *b*-type hemes with bishistidine ligation [116]. The two hemes are coordinated between transmembrane segments 2 and 5 in a manner reminiscent of, but distinct from, the heme coordination within mitochondrial complex III [117,118]. They have midpoint potentials of +125 mV (heme b_P) and +20 mV (heme b_D). Examination of the structure of NarI reveals two clefts, a larger one located between TM segments 1 and 2, and a small cleft located between TM segments 2 and 3.

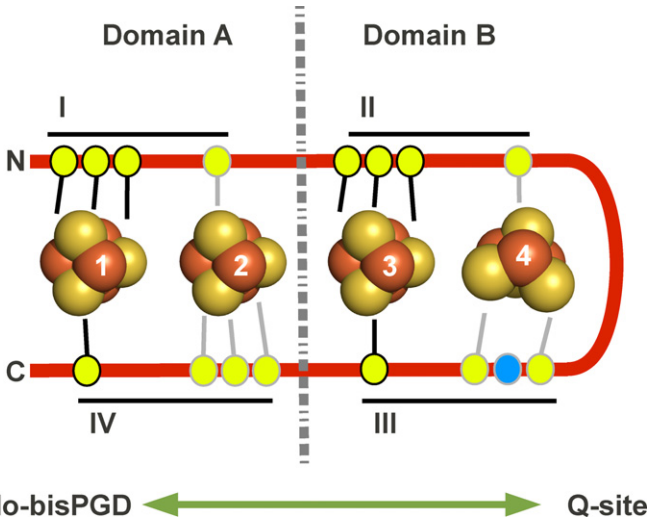

Fig. 5. Architecture of the four cluster protein subunit. The core architecture of the CISM four cluster protein subunit is predicted to result from a primordial gene insertion event resulting in one eight-iron ferredoxin domain being appended to another [35]. These are labelled as Domain A and Domain B in the figure. The resultant protein contains four Cysteine groups (I–IV) that coordinate the four [Fe–S] clusters (FS1–FS4) in the manner shown. Each cysteine residue is represented by a yellow circle, and the four [Fe–S] clusters are labelled 1–4 from left to right. For each Cysteine group, three Cysteine residues coordinate one [Fe–S] cluster, while the fourth coordinates the other [Fe–S] cluster of the pair. In the case of NarH, Cys group III has a Tryptophan residue at the second Cys position (C_B), and this is indicated as a blue circle in the figure. The Tryptophan substitution results in the assembly of a [3Fe–4S] cluster instead of a [4Fe–4S] cluster at the FS4 position. In almost all cases the four cluster protein subunit functions to provide part of an electron transfer relay connecting the Mo-bisPGD cofactor to a Q-site with the possibly involvement (in NarGHI) of an additional cluster in NarG (FS0) and two hemes in NarI (hemes b_P and b_D).

The observation of the two clefts suggested that there may be two quinone-binding sites, perhaps one for menaquinol and one for ubiquinol the two quinols utilized by NarGHI. However, extensive studies of the effects of two classical Q-site inhibitors, HOQNO (2-*n*-heptyl-4-hydroxyquinoline-*N*-oxide) and stigmatellin, as well as detailed pulsed EPR experiments with wild-type NarI and site-directed mutations of Lys86 and His66 in the quinol binding site indicate that menaquinol and ubiquinol binding occurs at a single site in the vicinity of the distal heme using a similar binding mode involving the His66 residue, a b_D heme ligand [5,119–121]. Quinol binding occurs in the vicinity of the heme oriented towards the periplasm, placing quinol oxidation close to the periplasmic side of the membrane, in agreement with the proposed bioenergetics of NarGHI and allowing the generation of a protonmotive force during turnover [35].

3.4. Family IV molybdoenzymes: the prokaryotic sulfite oxidase family (Fig. 2B)

Although this family primarily consists of sulfite oxidase of higher organisms and assimilatory nitrate reductase of plants, prokaryotic examples are known. The sulfite oxidase-fold (SUOX) enzymes are important in plant sulfite detoxification, agriculture, adaptation to pollution, and global geochemical cycles and the structures of several have been reported [47,122–126]. These enzymes mix and match a heme b_5 domain, a Mo-PPT binding SUOX-fold, a FAD-binding domain and a dimerization domain [127–129]. It is important to note that while the other three families of molybdoenzymes contain [Fe–S] clusters or interact with [Fe–S] subunits, members of Family IV do not. *Starkeya novella* sulfite oxidase (SorA) forms a stable dimer with a soluble cytochrome (SorB), which interacts transiently with a membrane-bound cytochrome c_{550} [124]. *T. thermophilus* SUOX, on the other hand, also interacts with a soluble cytochrome c, but only transiently [130].

Bioinformatic analyses of the *E. coli* genome identified the YedY protein (of the *yedYZ* operon) as a possible member of the sulfite oxidase class. This was confirmed by determination of the structure of YedY [41,131]. The *yedYZ* operon encodes a putative oxidoreductase with a soluble, periplasmic, MoPPT-containing catalytic subunit (YedY), and a heme-containing membrane-intrinsic subunit (YedZ). Mature YedY is 290 amino acid residues in length following cleavage of its N-terminal Tat leader, and is found in the periplasmic compartment. As predicted it contains the Mo-PPT form of the cofactor rather than the bis-dinucleotide form (Mo-bisPGD) found in the majority of bacterial molybdoenzymes. YedY comprises only the SUOX-fold, lacking the FAD and heme b_5 domains of sulfite oxidase [131]. YedY also lacks the Arg triad that stabilizes anionic substrates in SUOX fold enzymes [41]. The Mo of YedY is trapped in the Mo(V) state in its as-isolated form, and cannot be oxidized to Mo(VI) in potentiometric titrations. The redox partner of YedY is YedZ, a hydrophobic monoheme cytochrome b ($E_m = -8$ mV) [132] (low spin, bis-His coordination) with 6 predicted TM segments and a total of 211 amino acid residues. YedY interacts with YedZ and couples electrons to the membrane-intrinsic quinone pool [131].

4. Regulation of bacterial molybdoenzyme expression

Prokaryotic molybdoenzyme expression is controlled at three levels: Mo transport (Mo availability), cofactor biosynthesis and molybdoenzyme apo-protein expression by a complex array of overlapping transcription factors and a recently discovered riboswitch mechanism.

4.1. ModE, the molybdenum sensor

In *E. coli* and many other prokaryotes Mo is transported *via ModABC* which allows the bacteria to accumulate trace amounts of Mo from the environment [133]. *ModABC* is an ATP binding cassette (ABC) transporter composed of a periplasmic binding protein (ModA), a membrane subunit (ModB) and an ATPase (ModC). Earlier publications had suggested the presence of a fourth open reading frame, *modD*, but this was due to a frame shift sequencing error and the DNA in this region actually codes for the YbhA protein (a non-essential phosphatase) [134]. Binding of Mo by the ModE transcription factor results in a conformational change and ModE dimerization allowing the complex to bind to an upstream DNA sequence which contains an 8-base inverted repeat 5′-TAACGTTA-3′ flanked by two CAT boxes [135]. A combination of microarray and bioinformatic analyses of the *E. coli* genome has identified over 80 genes that are (or could be) regulated (induction or repression) by ModE-Mo [136,137]. ModE-Mo represses the expression of the *modABC* operon as might be expected if Mo is available [138]. ModE-Mo induces the *moaABCDE* operon that encodes enzymes which catalyze key steps in molybdopterin biosynthesis [135]. ModE also regulates the expression of the structural genes for many molybdoenzymes including periplasmic and membrane-bound nitrate reductase (*nap*, *narGHI*) and dimethyl sulfoxide reductase (*dmsABC*) [139,140].

4.2. Global regulation by FNR (fumarate nitrate regulation) and ArcA

As noted elsewhere in this review, part of the amazing respiratory diversity of prokaryotes results from the controlled expression of molybdoenzymes, under anaerobic growth conditions. The aerobic:anaerobic transition must be tightly controlled to optimize efficiency of substrate utilization. O_2 is the preferred acceptor,

followed by nitrate, trimethylamine-*N*-oxide$^-$ and dimethyl sulfoxide. The transition is controlled by the FNR transcription factor, the global regulatory protein whose activity is regulated by O_2 [141]. The *fnr* gene was originally identified as an activator of anaerobic respiratory gene expression by isolating pleiotropic mutants that lack most anaerobic respiratory pathways. FNR, a member of the very large FNR/Crp family of transcription factors [142], can both induce (e.g. *dmsABC*, *narGHJI*) and repress (e.g. *ndh*, *cyoABCDE*) operons in the FNR regulon [143,144]. FNR is composed of two domains: an N-terminal sensory domain with a Cys motif that coordinates a unique [4Fe–4S] cluster and a C-terminal domain with a helix-turn-helix motif that binds to a palindromic DNA sequence (NTTGAT). FNR contains four essential cysteines which coordinate an unstable [4Fe–4S] cluster. This cluster has a redox potential of about +400 mV, undergoes conversion from an active [4Fe–4S] state under anaerobic conditions (FNR dimer) to an inactive [2Fe–2S] cluster under aerobic conditions, *via* an intermediate [3Fe–4S] state. This transition is accompanied by the conversion of FNR from an active homodimer to an inactive monomer precluding DNA binding [145,146].

Another level of global regulation is achieved by the oxygen mediated ArcAB sensor kinase system [147]. The ArcA protein is a response regulator paired with a membrane-bound cognate sensor (histidine protein kinase) ArcB. The ArcA protein acts primarily as a transcriptional repressor of genes whose products are involved in aerobic metabolism [148]. ArcB protein controls ArcA protein activity through transphosphorylation reactions. Under aerobic conditions, the kinase activity of ArcB is inhibited by the quinone electron carriers that act as direct negative signals [149,150].

4.3. Response to nitrate and nitrite (NarXL and NarPQ)

Nitrate acts to induce the synthesis of *narGHJI* and simultaneously to repress the synthesis of other anaerobic respiratory chain components (e.g. *dmsABC*). The NarX–NarL two-component regulatory histidine/aspartate kinase phosphotransfer system detects and regulates gene expression in response to the availability of high concentrations of nitrate [148,149]. In *E. coli*, an alternative system, NarQ–NarP, activates gene expression in response to nitrate and is especially sensitive to low concentrations of nitrate [151]. Phosphorylation of the NarL and NarP response regulators is governed by the NarX and NarQ sensors in response to signal ligands, nitrate and nitrite. In *E. coli*, the NarX sensor is specialized for preferential response to nitrate, whereas the NarQ sensor is generalized for response to nitrate and nitrite. Evidence for an asymmetric signal-response cross-regulation network has recently been provided, in particular for the *narGHJI* operon such that NarQ interacts similarly with both response regulators, whereas NarX interacts preferentially with NarL [152]. When nitrate is present, expression of the genes for fumarate (*frdABCD*), trimethylamine-*N*-oxide (*torCAD*) and dimethyl sulfoxide reductases (*dmsABC*) is repressed while expression of the *narGHJI* genes is induced. Expression of the *nrfABCDEFG* (formate-dependent nitrite reductase) operon is repressed by the NarL protein in response to nitrate but activated by the NarL and NarP proteins in response to nitrite. All known NarL and NarP-regulated target operons are also controlled by FNR in response to anaerobiosis [153,154].

4.4. TorCAD regulation

Induction of the *torCAD* operon is controlled by anaerobiosis and trimethylamine-*N*-oxide in an unusual manner. Anaerobiosis induces expression but this is not under the control of FNR or ArcA. *torCAD* expression is also not affected by ModE [74]. Further, *torCAD* expression is not subject to the hierarchical control whereby substrates with higher redox potentials are preferentially induced. This regulation involves a two-component regulatory system comprising TorS, an unorthodox membrane-bound histidine kinase containing three phosphorylation sites and TorR a response regulator of the OmpR family [155,156]. The torT gene, located between torS and torR, is the third gene required for *torCAD* operon induction. TorT is a periplasmic protein where trimethylamine-*N*-oxide binding induces a cascade of conformational changes from TorT to TorS, leading to TorS activation [157].

In the TorSR system, TorI is a response regulator inhibitor that interacts with the effector domain of TorR, a region involved in binding RNA polymerase, without affecting TorR binding to DNA [158]. As a consequence, TorI limits TorR-mediated recruitment of RNA polymerase to the *torCAD* promoter and therefore acts as a negative regulator.

An additional level of regulation of *torCAD* is mediated by apo-TorC [159]. Immature TorC lacking the hemes, cannot interact with TorA but can interact with the periplasmic domain of TorS inhibiting the TorS kinase and thus negatively regulating expression of *torCAD*. This regulation is highly specific to apo-TorC and cannot be replaced by other immature c-type cytochromes. The regulation depends on the mono-heme carboxy-terminal domain of TorC and not on the tetra-heme amino-terminal domain.

4.5. The riboswitch

A new aspect of molybdoenzyme regulation has been the discovery of a highly conserved RNA motif located upstream of genes encoding Mo transport, Mo cofactor biosynthesis and molybdoenzymes in various prokaryotes including ©- and δ-proteobacteria, *Clostridia*, *Actinobacteria* as well as DNA from environmental samples. Riboswitches are ubiquitous in all kingdoms of life and regulate the expression of many genes involved in catabolism, anabolism, and the transport of various cellular metabolites [160]. They are often found in the untranslated regions of bacterial mRNAs where they regulate transcription elongation or initiation of translation. In *E. coli*, this RNA aptamer controls the *moaABCDE* operon (Moco biosynthesis) in response to cofactor production by binding Moco. Transcription of *moaABCDE* is upregulated by FNR and ModE, but translation of this operon is inhibited when free Moco is present. This ensures that Moco is synthesized only under conditions of anaerobicity (FNR) and sufficient molybdate (ModE), while preventing overproduction by binding free Moco. Furthermore, Moco RNA can discriminate between Moco and the W-containing analog [161].

5. The catalytic mechanism of molybdoenzymes

The mechanism of most prokaryotic molybdoenzymes is divided into two half cycles: an oxidative half in which reduced Mo(IV) binds the substrate and two electrons are transferred from Mo to the substrate. The second reductive half in which two protons and two electrons are transferred to Mo yielding H_2O and regenerating Mo(IV) [2]. While crystal structures for several members of the xanthine oxidase, sulfite oxidase, and dimethyl sulfoxide reductase families have provided considerable insight into how active site architecture dictates substrate specificity and reaction mechanism, this is still not fully understood [77,94]. In addition to the importance of conserved active site residues residing in substrate access funnels and binding pockets, atoms ligated to Mo function as catalytic players by virtue of their position and identity. For example in xanthine oxidase, a hydroxyl ligand functions as a nucleophile and is the source of oxygen transfer to substrate, while a sulfur atom is involved in handling protons [162]. It has recently been found that Mo ligands may also serve a protective role, such as the recently detected sulfur atom in the coordination sphere of DdNapA [93]. Computational investigation suggests that

this sulfur atom acts in concert with a cysteine from the protein to form a "pseudo-dithioline" group that protects the coordination sphere from solvent damage [163]. In this model, nitrate binding would cause conformational re-arrangement of the active site that displaces the pseudo-dithioline. An analogous system may exist in *E. coli* nitrate reductase A, where an aspartate ligand has been observed coordinating Mo with either one or both of its oxygens [4,46].

The role of the pterin portion of the cofactor and its specific contribution to reaction mechanism is another area of intense study. It is generally agreed that it primarily functions in metal positioning, redox potential modulation *via* its ring system, and transfer of electrons [162].

6. The role of molybdoenzymes in bioenergetics

As exemplified above, many prokaryotic molybdoenzymes are involved in the C, S and N cycles. In some cases, functioning of these enzymes (Family III only) is part of an anaerobic respiration process (for example, denitrification or anaerobic respiration of arsenic and selenium oxyanions) (see for reviews [164,165]). Schematically, the electrons released from the oxidation of a molecule by an electron donating enzyme are then passed *via* freely diffusible and lipophilic carriers, quinones, to electron-accepting enzymes. The electron transfer occurring throughout this multi-protein electron transport pathway is then associated with the net release of protons in the periplasmic compartment to generate a transmembrane electrochemical proton gradient or proton motive force (*pmf*). Such energetic coupling depends on the location of the active sites of respiratory enzymes. As reviewed above, a plethora of different cellular and subunit organizations exists among prokaryotic molybdoenzymes (Fig. 2) and as such, their functioning could either be electrogenic, electroneutral or even energy-dissipating. The paradigmatic example of the "redox loop mechanism" ($H^+/e^- = 2$) that derives from coupling two *pmf*-generating enzymes and cycling quinone/quinol between them is made up by two CISM enzymes from *E. coli*: formate dehydrogenase (FdnGHI) and the nitrate reductase (NarGHI) (see Fig. 2C) [4,6,101]. As evidenced recently, in archaea, the nitrate-reducing subunit NarG is periplasmic (pNarG in Fig. 2C), thanks to the presence of a Tat-signal peptide sequence at the N-terminus [166]. Moreover, the membranous cytochrome b subunit NarI is replaced by a soluble monomeric *b*-type one encoded within the operon. Such organization is shared by other Family III prokaryotic molybdoenzymes that function either as dehydrogenases (ethylbenzene and dimethylsulfide dehydrogenases) or as reductases (selenate and chlorate reductases). Finally, it has been suggested that nitrate reduction in the periplasm of archaea is electrogenic due to its association with a quinol-cytochrome c oxidoreductase complex [166]. Recently, it has been demonstrated biochemically that the same holds true for the selenate reductase from *Thauera selenatis* [167]. Examples of energy-dissipating molybdoenzymes can be seen with the periplasmic and soluble Dor/Tor or Nap enzymes, their roles being to serve turnover of the quinone/quinol pool to ensure a continuous supply of oxidized quinone for the quinone-reducing electron input components [168]. Although the structure of several prokaryotic molybdoenzymes are known, the electron transport chains that mediate electron transfer between the quinone pool to or from these termini are less well resolved and await further studies in a diverse range of prokaryotes.

7. Maturation of molybdoenzymes

As reviewed above, prokaryotic molybdoenzymes constitute a large and diverse group of metalloproteins harbouring several metal cofactors (hemes *b* and *c* [Fe–S] clusters) in addition to the Moco (Fig. 2). X-ray crystallographic studies of all known molybdoenzymes revealed that the Moco is not located at the surface of the protein but it is buried deeply within the enzyme and, in some cases, in close proximity to [Fe–S] clusters [4,6,34,38,82,97,106,131,169–172]. This observation suggests that Moco insertion is intimately connected to protein folding and subunit assembly.

Another consideration is that once Moco is liberated from the holoenzyme, it loses Mo and undergoes rapid and irreversible loss of function due to oxidation. The lability of the cofactor has limited elucidation of the biosynthesis of Mo-bisPGD and its incorporation into molybdoenzymes. It has been assumed that there is no free Moco present in the cell and it is either bound to a carrier protein that protects and stores Moco until further use or it is immediately transferred after biosynthesis to the apo-Mo-protein. Since the availability of sufficient amounts of Moco is essential for the bacterial cell to meet its changing demand for synthesizing molybdoenzymes the existence of a Moco-storage protein would be a good way to buffer supply and demand of Moco. In contrast to the green alga Chlamydomonas reinhardtii [173] or the plant Arabidopsis thaliana [174] where Moco-binding proteins shuttle synthesized Moco from the biosynthetic machinery to the apo-molybdoenzyme, in *E. coli* a complex of proteins involved in the final stages of Moco synthesis is in charge of Moco delivery to different apo-molybdoenzymes [175,176]. This process appears to be highly intricate and regulated and involves system-specific chaperones (see below).

To decipher the Moco incorporation step, several groups have used *in vitro* molybdoenzyme reconstitution assays. Completely defined *in vitro* systems for studying the mechanism of Moco insertion were established for dimethyl sulfoxide [177], trimethylamine-*N*-oxide reductases [178] and xanthine dehydrogenase [179]. However, these systems result in only partial activation even after several hours of incubation. The limited reconstitution is most likely due to the absence or inactivation of several necessary factors.

As described above the modular organization of many molybdoenzymes can involve multiple subunits and can be tethered to the cytoplasmic membrane often through *b*- or *c*-type cytochromes. The membrane subunits connect the cytoplasmic or periplasmic redox reactions with electron transport to or from the respiratory quinone/quinol pool. In addition to the Sec machinery, membrane insertion may require the help of the accessory protein YidC [180]. These enzymes can form subcomplexes of cytoplasmic subunits in the absence of the membrane anchoring subunits and these subcomplexes can retain oxidoreductase activity although this activity is uncoupled from electron transfer to or from the quinone/quinol pool. This suggests that the attachment of the enzymes to the membrane by their membrane anchor subunits is the last step in complex assembly. Within the prokaryotic cell, successful synthesis and assembly of molybdoenzymes is thus an intricate process that requires several steps such as the synthesis of the different subunits in the cytoplasm, their assembly, the incorporation of various types of metal or organic cofactors and the anchoring of the complex to the membrane. In the case of periplasmic or outer membrane molybdoenzymes [181], the assembly and metal cofactor incorporation steps takes place in the cytoplasm prior translocation across inner membrane *via* the Tat apparatus [69,71,182]. Importantly, system-specific chaperones often assist formation of active molybdoenzymes. In this context, Li et al. [183] reported the interaction of the system-specific chaperone DmsD with a number of general chaperones illustrating their more general participation in metalloenzyme maturation. Altogether, these system-specific and general chaperones may function to stabilize the substrates against mis-folding and proteolysis, such that a certain level of struc-

ture is acquired before Moco insertion can proceed, as well as to help escort Tat substrates to the translocon while preventing early engagement with the Tat machinery. Bacterial Tat systems export folded proteins including [Fe–S] containing proteins, partner subunits of most exported molybdoenzymes but also proofread these substrates. When Tat substrates are misfolded they are subjected to proteolysis, likely through a Tat-independent process [184–186]. Although it is most likely that all these events occur in a coordinate fashion to yield a final functional multimeric metalloprotein, information about how this coordination is performed is scarce. Most of the available information concerns members of the Family III (dimethyl sulfoxide reductase family) and Family II (XDH) and will be extensively described below. Concerning the maturation of Family I and Family IV enzymes, no enzyme-specific chaperones have been reported while the presence of several cofactors within the catalytic subunit or the periplasmic location of the enzyme preclude involvement of chaperones (see below).

7.1. Maturation of the Family III enzymes

7.1.1. The CISM group

7.1.1.1. The archetypal NarGHI-NarJ couple. *Ec*NarGHI [96] was one of the first molybdoenzymes whose maturation pathway was intensively studied. *Ec*NarGHI faces the cytoplasm and is a non-exported membrane-bound complex (c.f. Section 3.4). Initial biochemical and genetic studies indicated that the NarJ protein encoded by the *narGHJI* operon plays an essential role in nitrate reductase activity promoting correct assembly of the enzyme complex without being part of the final structure [24]. Based on these properties, a role as a private or system-specific chaperone was proposed [24]. *E. coli* synthesizes a second nitrate reductase complex, the NarZYV isoenzyme, whose maturation involves the NarW protein, a NarJ homologue, that is interchangeable with NarJ [187]. The X-ray structure of a NarJ-like protein from Archaeglobus fulgidus indicates an all-helical fold (PDB ID code 2o9x) [188], a feature shared by other bacterial system-specific chaperones such as DmsD (PDB ID codes: 1s9u, efp, 3cw0) or TorD (PDB ID code 1n1c) [189–191], thus forming a new family of chaperones (Pfam PF02613) (Fig. 6).

NarGHI assembly is complex and intricate. Recent progress in the functions associated with the NarJ chaperone has provided significant insights into this process [109,192]. Two distinct NarJ-binding sites were mapped on the NarG catalytic subunit, one of them corresponding to the N-terminus [193]. NarJ binding to this region represents part of a chaperone-mediated quality control process preventing membrane anchoring of the soluble and cytoplasmic NarGH complex before all maturation events have been completed. In particular, NarJ ensures complete maturation of the *b*-type cytochrome NarI by proper timing for membrane anchoring of the cytoplasmic NarGH complex [109]. This process strongly resembles the "Tat proofreading" of periplasmic metalloproteins, of which the best-studied example relates to *E. coli* *Ec*TorA (see Section 3.3.1) [194]. A similarity between the Tat signal peptides and the N-terminus of the non-exported NarG [195] has recently been examined by Ize et al. [196] who found that a limited number of amino acid substitutions allow the N-terminus of NarG to direct translocation of fused proteins by the Tat translocon. Moreover, in archaea and some bacteria, the NarG sequence harbours a typical Tat signal peptide responsible for the periplasmic localization of the NarGH complex [166]. A combination of biophysical approaches allowed the basis of recognition between NarJ and the N-terminus of NarG to be deciphered. NMR structural analysis demonstrated that the N-terminus of NarG adopts a helical conformation in solution which remains largely unchanged upon NarJ binding [192]. Moreover, NarJ recognizes and binds the helical $NarG_{1-15}$ peptide within a highly conserved and elongated groove mostly *via* hydrophobic interactions [25,192]. Isothermal titration calorimetry and BIAcore experiments support a model whereby the protonated state of the chaperone controls the time dependence of peptide interaction [192]. Interestingly, NMR and differential scanning calorimetry analysis revealed a modification of NarJ conformation during complex formation with the $NarG_{1-15}$ peptide. Such a structural flexibility of the chaperone appears to be a common feature of several members of this new family of chaperones as deduced from the observation of several disordered regions [188,189,197]. As reported recently, different folding forms of the *Ec*TorA specific chaperone TorD are associated with different biological activities [198]. The function of these chaperone proteins is not restricted to the recognition and binding of the N-terminus of the nascent metalloprotein, but includes their participation in metal cofactor insertion processes through additional contacts with their specific partner.

An undefined NarJ-binding site within the catalytic subunit NarG is responsible for sequential insertion of the proximal [Fe–S] cluster (FS0) and of the Mo-bisPGD [109]. Indeed, FS0 insertion must precede Mo-bisPGD insertion as recently confirmed by X-ray structural analysis of specific mutants of the FS0 coordination sphere [110]. While the lack of Mo-bisPGD does not preclude FS0 insertion, substitution of cysteine ligands of the FS0 cluster or the absence of NarJ prevents insertion both of FS0 and of Mo-bisPGD [105,110,120]. The exact function of NarJ in this process is unclear. Nevertheless, NarJ is an indispensable component of the Mo-bisPGD insertional process in authorizing the interaction of apoNarGH with a complex made up of several cofactor biosynthetic proteins in charge of Mo-bisPGD delivery [176].

In the absence of NarJ, a global defect in metal incorporation into NarGHI is observed. In addition to both metal cofactors of the catalytic subunit NarG, the proximal heme b_P is absent due to loss of coordination between maturation of the NarI and NarGH components [109]. Finally, the absence of NarJ did not appear to affect the stability or the cellular distribution of the apoenzyme which remains largely associated to the cytoplasmic membrane [23,193]. An explanation may derive from the analysis of the apoNarGHI structures lacking either the Mo-bisPGD (PDB ID code 1siw) [105] or both FS0 and Mo-bisPGD (PDB ID code 3ir6) [110]. In both cases, GDP moieties can be inserted into positions corresponding to GDP-P and GDP-D, thus conferring a relative structural stability of the enzymatic complex [105,110]. Such a situation has also been encountered in the case of the CO dehydrogenase from *H. pseudoflava* expressed from tungstate-grown cells [199] or in the case of the *Rh*DorA protein heterologously expressed in a Mo-bisPGD deficient *E. coli* strain [177]. One could envision that the chaperone either catalyzes the rapid exchange of the nucleotides for Mo-bisPGD or prevent nucleotide insertion through direct contacts with the metalloenzyme. Protonation of a specific residue of NarJ increases the affinity towards the N-terminus of NarG, in particular *via* the lifespan of the complex [192]. A tentative model for the physiological NarJ chaperone cycle can be deduced from these data and initiates with the rapid binding of the N-terminus of NarG by the protonated chaperone at high affinity ($K_d \sim 3$ nM) followed by its release by a deprotonated chaperone at lower affinity ($K_d \sim 0.1$ μM) and reduced lifespan once cofactor loading and protein folding are complete. The nature of the signal that may trigger dissociation of the complex remains unclear; however, preliminary results from structural analysis of the apo-Mo-NarGH complex produced in the absence of NarJ are consistent with a substantial conformational change of NarG allowing access to the interior of the protein to metal cofactors (A. Magalon, unpublished data). Structural modifications associated with metal cofactor insertion within NarG may thus be responsible for NarJ dissociation from the N-terminus.

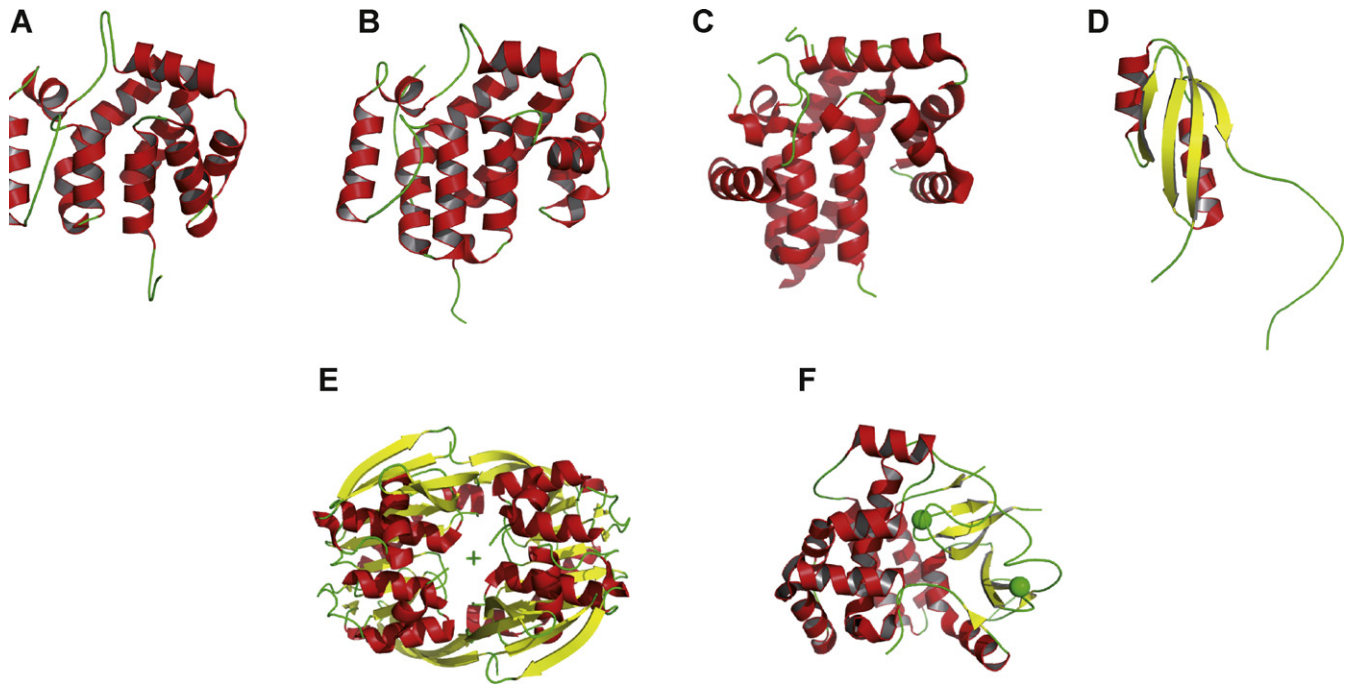

Fig. 6. Structure of different molybdoenzyme-specific chaperones. (A) NarJ from Archaeoglobus fulgidus (PDB ID code 2o9x) [188]. (B) DmsD from *Escherichia coli* (PDB ID code 3EFP) [203]. (C) TorD monomer from *Shewanella massilia* (PDB ID code 1n1c) [189]. (D) NapD from *Escherichia coli* (PDB ID code 2jsx) [219]. (E) FdhD dimer from *Desulfotalea* psychrophila (PDB ID code 2pw9). (F) FdhE from *Pseudomonas aeruginosa* (PDB ID code 2fiy). Individual figures were generated with PYMOL [256] by using the deposited coordinates from the protein structure database (http://www.pdb.org). The proteins are represented in cartoon with α-helices colored in red and β-sheets colored in yellow. A sulfate is co-crystallized with FdhD (green cross at the center of the dimer) while two iron atoms are coordinated by FdhE (represented by green spheres).

Altogether, these data demonstrated that NarJ orchestrates metal cofactor insertion, subunit assembly, and membrane-anchoring steps during the maturation of the NarGHI complex (Fig. 7). NarJ proofreads metal center insertion within the catalytic subunit prior to membrane anchoring through binding to a remnant Tat signal peptide. The underlying mechanism described herein is comparable to the one which occurs during translocation of Tat substrates. Importantly, it can be inferred from comparison with other multimeric molybdoenzymes that the multiple functions played by NarJ in the biogenesis process of the nitrate reductase complex

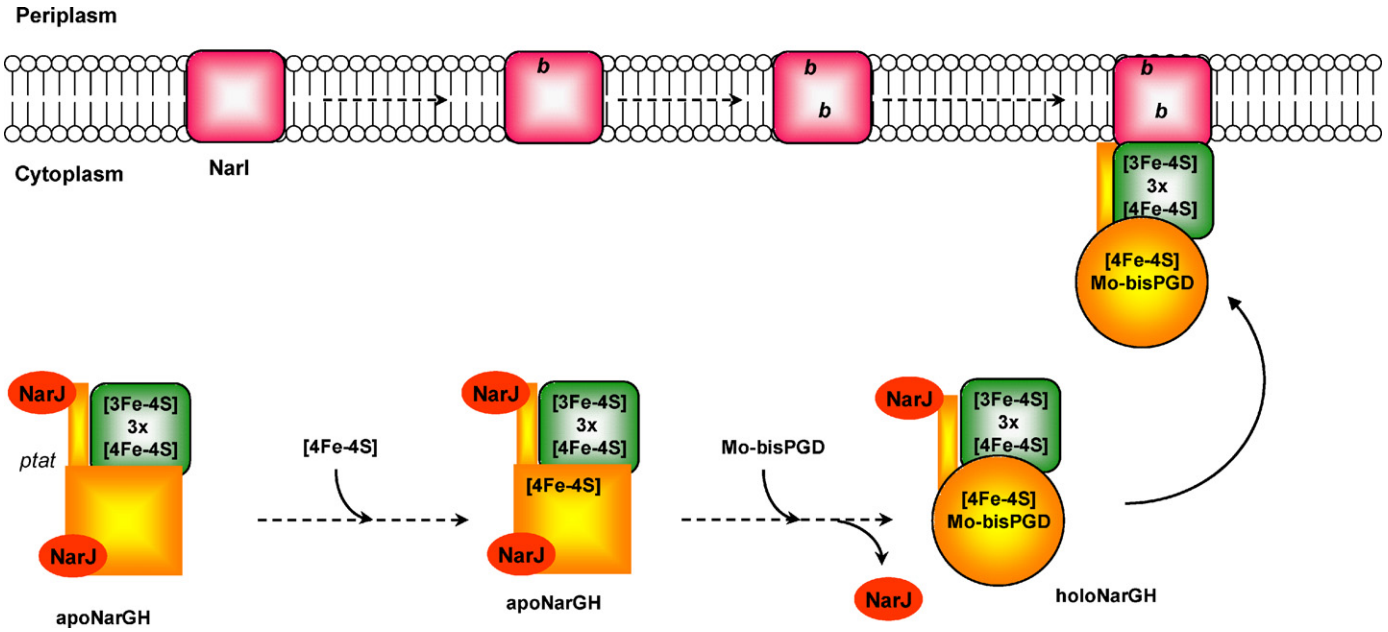

Fig. 7. Biogenesis model of the *E. coli* nitrate reductase A (NarGHI) complex. NarG and NarH constitute the catalytic dimer, while NarI is the *b*-type membrane anchor subunit of the complex. NarI maturation takes place in the inner membrane where the two *b*-type b_D and b_P hemes are sequentially inserted. [3Fe–4S] and 3x [4Fe–4S] clusters are likely inserted in the NarH subunit co-translationally through the action of one of the [Fe–S] biosynthetic machineries followed by the formation of an apoNarGH complex. This complex intermediate is specifically targeted by the enzyme-specific chaperone NarJ yielding a [NarJ–apoNarGH] maturation complex. NarJ interacts with the N-terminal of NarG (*ptat*) that is strongly related to a Tat signal peptide and as such, avoids premature membrane anchoring of the immature apoNarGH complex. NarJ interaction to a second site allows sequential insertion of the [4Fe–4S] cluster, FS0 and of the Mo-bisPGD cofactor within the catalytic subunit NarG. Conformational changes of the catalytic NarGH dimer upon insertion of the metal centers is likely responsible for NarJ dissociation and membrane binding of the mature NarGH complex.

Tat signal peptide Binding

Chaperone	*Target*	*Microorganism*	*Reference*
NarJ	NarG*	*E. coli*	[192]
TorD	TorA	*E. coli*	[194]
DmsD	DmsA	*E. coli*	[200]
NapD	NapA	*E. coli*	[219]
DdhD	DdhA	*R. sulphidophilum*	Predicted
EbdD	EbdA	*Azoarcus sp.*	Predicted
ClrD	ClrA	*I. dechloratans*	Predicted

[Fe-S] insertion

Chaperone	*Target*	*Microorganism*	*Reference*
NarJ	NarG	*E. coli*	[109,110]
NapF	NapA	*E. coli*	[221]
DmsD	DmsA	*E. coli*	Predicted
DdhD	DdhA	*R. sulphidophilum*	Predicted
EbdD	EbdA	*Azoarcus sp.*	Predicted
ClrD	ClrA	*I. dechloratans*	Predicted

Molybdenum cofactor binding

Chaperone	*Target*	*Microorganism*	*Reference*
TorD	TorA	*E. coli*	[228]
XdhC	XdhA	*R. capsulatus*	[179]
XdhC-like	QroL	*P. putida*	Predicted

Molybdenum cofactor sulfuration

Chaperone	*Target*	*Microorganism*	*Reference*
XdhC	XdhA	*R. capsulatus*	[232]
XdhC-like	QroL	*P. putida*	Predicted

Unknown function

Chaperone	*Target*	*Microorganism*	*Reference*
FdhE	FdnG	*E. coli*	[215,217]
FdhD	FdnG,FdhF	*E. coli*	[215]

Fig. 8. The four functions of enzyme-specific chaperones. Chaperones fulfil (as referenced) or are predicted to fulfil one or several functions in prokaryotic molybdoenzymes maturation. (1) Tat signal peptide binding refers to interaction of the chaperone with the Tat signal peptide or to a strongly apparented one (indicated with an asterisk). (2) [Fe–S] insertion refers to requirement of the chaperone for [Fe–S] cluster insertion within the Moco-containing catalytic subunit. (3) Molybdenum cofactor binding refers to the ability of the chaperone to bind and deliver Moco to the molybdoenzyme. (4) Molybdenum cofactor sulfuration refers to the ability of the chaperone to bind and sulfurate Moco prior its insertion within the molybdoenzyme. (5) Unknown function refers to chaperones for which not sufficient data is available to ascertain their exact function. *E. coli*, *Escherichia coli*; *R. sulphidophilum*, *Rhodovulum sulphidophilum*; *T. selenatis*, *Thauera selenatis*; *I. Dechloratans*, *Ideonella dechloratans*; *R. capsulatus*, *Rhodobacter capsulatus*; *P. putida*, *Pseudomonas putida*.

will be extended to other related systems (Fig. 8). Indeed, the phylogenetic tree from sequence comparison of the catalytic subunit of all known archaeal and bacterial molybdoenzymes belonging to the dimethyl sulfoxide reductase family indicates that all contain a [Fe–S] cluster in close proximity to the Mo-bisPGD with the exception of a small clade including DorA/TorA/BisC enzymes only present in proteobacteria [35]. This taxonomic distribution indicates that the entire group of DorA/TorA/BisC enzymes arose at a late stage on the microbial evolutionary timescale. Accordingly, their enzyme-specific chaperones (with TorD as prototype) may have lost the function associated with the strict requirement in FS0 insertion prior to Mo-bisPGD as seen in NarJ. Alternatively, folding and assembly of those molybdoenzymes containing both a [Fe–S] cluster and a Mo-bisPGD in their catalytic subunit may rely on the functions of system specific chaperones with NarJ as a prototype.

7.1.1.2. The periplasmic CISM. *Ec*DmsABC and *Ec*FdnGHI, two periplasmically oriented and membrane-bound heterotrimeric complexes share strong similarities in terms of subunit and redox cofactor composition with the nitrate reductase complex (Fig. 2C) and may follow the same folding and assembly pathways and be assisted by a system-specific chaperone sharing functional simi-

larities to NarJ. Oresnik et al. reported that DmsD is essential for the assembly of a fully active DmsABC complex [200]. The *dmsD* gene (formerly *ynfI*) is part of the *ynf* operon encoding putative Tat-targeted selenate reductases [69,201]. Interestingly, DmsD ensures the folding and assembly of both the DmsABC and the two putative selenate reductases which contrasts with the usual exquisite specificity displayed by the so-called system-specific chaperones [201,202]. The strong sequence similarity of the corresponding catalytic subunits may explain such behaviour. X-ray structural analysis of DmsD from *E. coli* (PDB ID codes 3efp and 3cw0) [191,203] and *S. typhimurium* (PDB ID code 1s9u) [190] indicate an all-helical architecture as in NarJ and TorD. DmsD displays a structural plasticity as revealed by the existence of different folding forms [197] or of a disordered loop in the X-ray data [190]. Further, DmsD was isolated as a protein binding the Tat signal peptide of DmsA [200] and its ability to interact with two components of the Tat translocase, namely TatB and TatC located in the inner membrane, suggests a role in delivering the DmsAB substrate to the TatBC receptor complex [204,205]. More recently DmsD has been shown to interact with general chaperones and with several Moco biosynthesis proteins extending its interactome [183]. Combining random and site-directed mutagenesis on *E. coli* DmsD, a pocket of surface residues important for signal peptide binding was modelled [206]. This putative signal peptide binding site is made up of sections of three conserved loops and is predominantly hydrophobic [203]. Microcalorimetric analysis of peptide binding by either NarJ, DmsD or TorD chaperones provide further support to the hydrophobic character of the interaction [192,197,207]. Docking calculations with the solved structure of the N-terminus of NarG points towards a highly conserved and elongated hydrophobic groove in NarJ which partly overlaps with the hot pocket mentioned above [192]. Finally, deletion of the DmsA signal peptide results in the formation of a less stable but soluble and cytoplasmically active DmsAB complex [68]. Accordingly, the DmsA variant has likely benefited from the action of DmsD to a second unidentified binding site. Concerted action of DmsD on both the signal peptide and most likely to a second site of the DmsA protein, in the same way as NarJ, is thus required for productive synthesis of DmsABC. Detailed analysis of the metal cofactors insertion step driven by DmsD is yet to be fully understood.

A number of periplasmic or periplasmically oriented multimeric molybdo-enzymes of the dimethyl sulfoxide reductase family have been genetically or biochemically characterized in different bacteria or archaea such as the selenate [208], nitrate [166], chlorate [83] or perchlorate [86] reductases and the ethylbenzene [209] or dimethylsulfide [85] dehydrogenases. Considering their relatedness to the NarGHI or DmsABC complexes and the existence of an additional gene encoding for a NarJ/TorD/DmsD-like chaperone protein in the corresponding operons, it is tempting to speculate that folding and assembly of these molybdoenzymes will follow the same trend (Fig. 8). Exceptions are the periplasmic and multimeric arsenite oxidase (Aox), polysulfide (Psr) and arsenate reductase (Aro) enzymes which do not possess in their respective operons an additional gene encoding for a system-specific chaperone [165,210]. However, the presence of a Tat signal peptide and of a [Fe–S] cluster together with the Mo-bisPGD in the catalytic subunit supports the hypothesis that their maturation pathway will need assistance by an as yet unidentified system-specific chaperone which may be located elsewhere in the genome.

E. coli synthesizes three formate dehydrogenase isoenzymes. Two of these, are periplasmically oriented membrane-bound respiratory complexes, namely, the nitrate-inducible FdnGHI and the constitutively expressed cryptic FdoGHI [6,211]. Typical Tat signal peptides are present on the FdnG and FdoG catalytic subunits. The third isoenzyme, composed of a single cytoplasmic subunit (FdhF), is part of the formate hydrogenlyase complex [38,212]. All three isoenzymes harbor a [4Fe–4S] cluster in addition to the Mo-bisPGD cofactor in their catalytic subunit. Genetic studies have demonstrated that both *fdhD* and *fdhE* genes, located astride the *fdo* operon, are involved in the formation of active formate dehydrogenase enzymes, *fdhE* being restricted to periplasmic ones [213–216]. Interestingly, FdhD and FdhE do not share any structural similarity with other system-specific chaperones such as NarJ/TorD/DmsD. FdhD contains several cysteine residues and displays a mostly helical architecture [195] as confirmed by the resolution of the crystal structure of FdhD from *Desulfotalea psychrophila* (PDB ID code 2pw9). FdhE is an iron-binding rubredoxin which possesses four conserved CX_2C motifs essential both for FdhE stability and biological function [217]. As disclosed by the crystal structure at 2.1 Å of FdhE from *Pseudomonas aeruginosa* PAO1 (PDB ID code 2fiy), each two pairs of CX_2C motifs located in disordered loops coordinate an iron atom with an as yet unclear role. Interestingly, FdhE interacts both with the FdnG and FdoG catalytic subunits [217] while FdhD interacts with the cysteine desulfurase IscS, a key player in [Fe–S] cluster biosynthesis or selenocysteine incorporation within the catalytic subunit of formate dehydrogenases [218]. Nevertheless, the biological functions associated with both FdhD and FdhE in the formation of active formate dehydrogenases remain unclear and await further studies.

As in the case of the *E. coli* formate dehydrogenases, folding and assembly of the periplasmic nitrate reductase (NapAB) involves two cytoplasmic proteins, NapD and NapF, which do not display any sequence or structure similarity with other system-specific chaperones. Maillard et al. [219] reported that *E. coli* NapD displayed a ferredoxin-type fold and is involved in Tat signal peptide binding [219], NapF interacts directly with the catalytic subunit NapA, and may be involved in NapA folding and assembly prior to export *via* the Tat translocon [220]. *R. sphaeroides* NapF harbours four conserved tetra-cysteine motifs coordinating labile [Fe–S] clusters supporting its involvement in [Fe–S] cluster insertion within the catalytic subunit NapA. This provides further evidence of an active role of NapF in metal center insertion [221]. Recently, Kern and Simon reported that a *napF* knockout mutant accumulates the inactive cytoplasmic NapA precursor in *Wolinella succinogenes* [222]. However, there are many examples of organisms that lack *napF* such as *Campylobacter* species. One may envision that the *napF* gene has been lost during evolution if it is functionally redundant in the cell.

7.1.2. Family III enzymes with only a Mo-bisPGD cofactor: the archetypal TorA-TorD couple

While biogenesis of multimeric molybdoenzymes harbouring a [Fe–S] cluster and a Mo-bisPGD in the catalytic subunit appears to be intricate and requires a system-specific chaperone, what is the situation in those monomeric molybdoenzymes (TorA/DorA/BisC) harbouring Mo-bisPGD as sole prosthetic group? Among them, BisC is the unique non-exported molybdoenzyme and it is unclear whether Moco insertion is assisted by a system-specific chaperone. Conversely, formation of an active and periplasmically localized TorA/DorA enzyme relies on the action of system-specific chaperones.

In *E. coli*, reduction of trimethylamine-*N*-oxide is primarily catalyzed by expression of the inducible *torCAD* operon [65,223]. The terminal reductase, TorA, is a periplasmic molybdoenzyme harbouring Mo-bisPGD as the sole prosthetic group [78]. The last gene of the *tor* operon, *torD*, encodes a cytoplasmic private chaperone of TorA. Pommier et al. [224] reported that, in a *torD* knockout mutant, the activity and stability of a correctly localized TorA is strongly affected. Furthermore, the remaining enzyme is fully degraded under thermal stress conditions, Moco deficiency or molybdenum starvation [225]. Instability of the apo-molybdoenzyme is also observed with *Rhodobacter capsulatus* DorA, in the absence

of the system-specific chaperone DorD [226]. These observations differ markedly from the multimeric nitrate reductase where the absence of the NarJ chaperone does not significantly affect the stability and the cellular localization of the enzyme complex [23,193]. An explanation can be provided by the initial formation of a stable apo-Mo-NarGH complex prior to the action of NarJ compared to the monomeric DorA/TorA enzymes. Interestingly, the TorD chaperone from *S. massilia* forms multiple and stable oligomeric species and has been crystallized as a dimer with domain swapping between the two monomers having an all-helical fold (PDB ID code 1n1c) [189,227].

As in the case of NarJ, TorD interacts on two distinct sites of the TorA enzyme, one of them being the twin-arginine signal peptide located at the N-terminus [207,228]. This property is a general principle for this new class of chaperones (Pfam PF02613). Considering the periplasmic location of the TorA enzyme and the fact that Moco incorporation is a strictly cytoplasmic event, it is important that export is prevented until all assembly processes are complete. One of the mechanisms that ensures proper coordination between cofactor insertion and export is based on the ability of the chaperone to shield the signal peptide from interaction with the Tat translocase until Moco insertion [194]. This mechanism is reminiscent of the protection of the N-terminus of NarG by NarJ to allow proper timing for membrane anchoring of the soluble NarGH [109,193]. Interestingly, while TorD has a weak affinity for GTP ($K_d \sim 370\,\mu M$) which is enhanced by signal peptide binding [207], only the dimeric form displays a low intrinsic magnesium dependent GTP hydrolysis activity despite the absence of classical nucleotide-binding motifs [198]. The role of nucleotide binding or hydrolysis in modulating the interaction between the signal peptide and TorD remains unclear. Alternatively, Genest et al. reported TorA signal peptide protection by TorD regardless of the presence of Moco and or the Tat translocase [229]. At this stage, it is not clear whether TorD binding to the signal peptide monitors the folding and assembly of the substrate, or alternatively, retards the export kinetics sufficiently to allow completion of the Moco insertion process.

A second TorD-binding site was established on the core of the TorA enzyme and is responsible for a conformational change of the latter [224]. Using an *in vitro* system, Ilbert et al. [178,230] demonstrated that Mo-bisPGD insertion within apo-TorA is strongly facilitated by the presence of TorD and that deletion of the signal peptide has no significant effect as judged by TorA activity. Exquisite specificity is observed during this process as none of the TorD homologs can replace it. Binding to the core of TorA appears to be necessary for maturation and is mediated by helix 5 of TorD [228]. Recently, TorD was shown to interact with Moco biosynthesis components, including MobA, and Mo-PPT [228]. The authors suggest that TorD, while being dispensable, acts as a platform connecting the last step of the synthesis of the Mo-bisPGD just before its insertion into the catalytic site of TorA. The immediate question raised by these observations is whether this role is shared by other system specific chaperones. In the case of NarJ, a strict requirement of the chaperone has been observed for FS0 insertion within the catalytic subunit, a step that must precede Mo-bisPGD insertion, a clear distinction from TorD. Nevertheless, it cannot be discounted that upon FS0 insertion, NarJ has an active role in facilitating Moco insertion. An answer to this question awaits further studies.

7.2. Maturation of Family II enzymes

A clear distinction between the sulfite oxidases (Family IV) and xanthine dehydrogenases (Family II) is the presence of a sulfur atom on the Mo coordination sphere in the latter (see Section 3.2). A conserved post-translational mechanism from bacteria to eukaryotes for Moco sulfuration has been studied in detail during the last decade where a Moco-binding protein through direct interaction with a cysteine desulfurase, ensures both the sulfuration step of the cofactor and its protected transfer to the apo-molybdoenzymes. While in eukaryotes the two components are fused into a single polypeptide, also called Moco sulfurase [231], this is not the case in prokaryotes where a system-specific chaperone is operating together with a cysteine desulfurase [179,232]. While the sequence analysis of archaeal genomes indicate the presence of xanthine dehydrogenase, the mechanism of Moco sulfuration has not yet been studied.

We will review the incorporation of sulfurated Mo-PPT by using the best-studied system, the *Rhodobacter capsulatus* xanthine dehydrogenase. This enzyme consists of a cytoplasmic heterodimeric complex ($\alpha_2\beta_2$) that catalyzes the hydroxylation of hypoxanthine and xanthine, the last two steps in purine degradation [39]. The XdhA subunit contains two [2Fe–2S] clusters in addition to FAD, while the XdhB subunit binds Mo-PPT [59] as confirmed by the crystal structure [44]. Functional synthesis of the *R. capsulatus* XdhAB complex requires the presence of a system-specific chaperone, XdhC, encoded by the *xdhABC* operon which entails binding of Mo-PPT and its insertion into the XdhB subunit [233]. In that sense, XdhC differs considerably from the above-mentioned system-specific chaperones for Mo-bisPGD containing enzymes (Family III) as it does not proofread its metalloenzyme substrate. XdhC specifically promotes the sulfuration of Moco by interaction with a cysteine desulfurase, which transfers the sulfur to Moco bound to XdhC, an oxygen-sensitive process [179,232]. In this context, XdhC was shown *in vitro* to tightly bind PPT in stoichiometric amounts and, as such, protects the sulfurated form of PPT from oxidation before its transfer into apoXdhAB through a direct protein interaction with the catalytic subunit XdhB [179]. Importantly, to prevent all available Moco in the cell from being converted to Mo-bisPGD and to guarantee a Mo-PPT supply for XdhAB, XdhC interacts with MoeA and MobA proteins involved in the final stages of Moco synthesis. Whereas interaction with MoeA allows Moco transfer to XdhC, its interaction with MobA, in charge of nucleotide addition to the PPT moiety, prevents the binding of Moco to the latter simultaneously inhibiting PGD formation [232]. Considering the structure of the heterotetrameric enzyme and the presence of three different metal centers, biochemical and biophysical studies revealed that assembly of XdhAB is a multistep process which occurs in an ordered manner. It involves the synthesis and interaction of both subunits, followed by [Fe–S] cluster and FAD insertion within XdhA, dimerization of the XdhAB complex, and finally, insertion of sulfurated Moco into XdhB, resulting in an active enzyme [234]. Such a model is reminiscent of the nitrate reductase complex where formation of a [Fe–S] clusters loaded NarGH complex should precede Moco insertion [109]. A notable difference is that XdhC plays no active role in orchestrating this assembly process in contrast with NarJ.

8. Future perspectives

As detailed in this review, the last decade has seen enormous progress in our understanding of the structure, function and maturation of molybdoenzymes. This has resulted from the growing success of membrane protein crystallography together with the application of sophisticated genetic, biophysical, biochemical and bioinformatical methodologies. However, most of the data concentrate on the Families II and III which represent to date the largest groups of prokaryotic molybdoenzymes. Many significant questions remain to be elucidated.

1. Why do most prokaryotic molydoenzymes have a bis-pterin cofactor? This is a complex and expensive (in terms of cellular

metabolism) cofactor to synthesize. Do the P and D pterins serve different roles in catalysis?
2. Members of the CISM group of enzymes (e.g. dimethyl sulfoxide reductase and nitrate reductase) have a very low potential cluster as an essential member of the electron transfer relay. Does this cluster serve a role in modulating catalysis?
3. How does the active site architecture determine substrate specificity, enzyme reactivity and stereochemistry? Considering the heterogeneity of the active site observed by EPR spectroscopy, more efforts must be put to identify the corresponding structures by means of DFT calculations for instance.
4. What is the detailed mechanism of Moco insertion into target enzymes? In this context, what is the exact function played by the dedicated chaperone or the rational behind their systemic occurrence for some molybdoenzymes such as NarGHI?
5. How can the several distinct functions for those dedicated chaperones, with only a single X-ray crystal structure, be reconciled?
6. Does the assembly of all prokaryotic molybdoenzymes require the action of a dedicated chaperone? The same holds for eukaryotic counterparts whose assembly is poorly understood. Extending the maturation studies to members of other families is thus required to get an overall view and to draw general principles which would govern assembly of prokaryotic molybdoenzymes.
7. X-ray data revealed an oligomeric organization of respiratory molybdoenzymes in several cases and formation of supercomplexes is proposed. How such quaternary organization of the enzymatic complexes is regulated by the bacterial cell in response to metabolic demand or changing environments?
8. The explosion of genome sequencing projects has identified several yet uncharacterized molybdoenzymes which may catalyze unique chemical transformations that may prove useful in synthetic biology applications. Furthermore, genomic data combined to in-depth phylogenetic and biochemical analyses of molybdoenzymes and of their dedicated chaperones (when known) could provide a clear-cut evolutionary scheme that in turn will not only favourably complement the structural work done on enzymes to define the evolutionary diversification of the entire family but also allow better understanding of assembly processes.

Acknowledgements

The authors wish to thank Dr. Richard Rothery and Matthew Solomonson for their help in the preparation of this review. The authors wish to thank group members and B. Guigliarelli, S. Grimaldi, C. Léger, D. Pignol, P. Arnoux, W. Nitschke, B. Schoepp-Cothenet, R.R. Mendel and F. Bittner for stimulating discussions and collaborations on Moco-containing enzymes. Work in the JHW laboratory was supported by the Canadian Institutes of Health Research and Alberta Innovates: Health Solutions. Work in the AM laboratory was supported by the CNRS, Aix-Marseille University and the ANR.

References

[1] R. Hille, Trends Biochem. Sci. 27 (2002) 360.
[2] C. Kisker, H. Schindelin, D.C. Rees, Annu. Rev. Biochem. 66 (1997) 233.
[3] A. Kletzin, M.W. Adams, FEMS Microbiol. Rev. 18 (1996) 5.
[4] M.G. Bertero, R.A. Rothery, M. Palak, C. Hou, D. Lim, F. Blasco, J.H. Weiner, N.C.J. Strynadka, Nat. Struct. Biol. 10 (2003) 681.
[5] M.G. Bertero, R.A. Rothery, N. Boroumand, M. Palak, F. Blasco, N. Ginet, J.H. Weiner, N.C.J. Strynadka, J. Biol. Chem. 280 (2005) 14836.
[6] M. Jormakka, S. Törnroth, B. Byrne, S. Iwata, Science 295 (2002) 1863.
[7] L.E.P. Dietrich, M.M. Tice, D.K. Newman, Curr. Biol. 16 (2006) R395.
[8] D.R. Lide, CRC Handbook of Chemistry and Physics, 90th ed., CRC Press, 2009.
[9] J.R. Andreesen, K. Makdessi, Ann. N. Y. Acad. Sci. 1125 (2008) 215.
[10] M. Leslie, Science 323 (2009) 1286.
[11] R.J.P. Williams, R.J.P. Williams, J.J.R.F.D. Silva, The Chemistry of Evolution: The Development of Our Ecosystem, Elsevier, 2006.
[12] A.D. Anbar, A.H. Knoll, Science 297 (2002) 1137.
[13] D. Fike, Nat. Geosci. 3 (2010) 453.
[14] P.L. Hagedoorn, W.R. Hagen, L.J. Stewart, A. Docrat, S. Bailey, C.D. Garner, FEBS Lett. 555 (2003) 606.
[15] J. Buc, C.L. Santini, R. Giordani, M. Czjzek, L.F. Wu, G. Giordano, Mol. Microbiol. 32 (1999) 159.
[16] J.L. Johnson, K.V. Rajagopalan, J. Biol. Chem. 251 (1976) 5505.
[17] A. Sevcenco, L.E. Bevers, M.W.H. Pinkse, G.C. Krijger, H.T. Wolterbeek, P.D.E.M. Verhaert, W.R. Hagen, P. Hagedoorn, J. Bacteriol. 192 (2010) 4143.
[18] S. Rech, U. Deppenmeier, R.P. Gunsalus, J. Bacteriol. 177 (1995) 1023.
[19] S. Rech, C. Wolin, R.P. Gunsalus, J. Biol. Chem. 271 (1996) 2557.
[20] J. Nichols, K.V. Rajagopalan, J. Biol. Chem. 277 (2002) 24995.
[21] J.D. Nichols, S. Xiang, H. Schindelin, K.V. Rajagopalan, Biochemistry 46 (2007) 78.
[22] L.E. Bevers, P. Hagedoorn, J.A. Santamaria-Araujo, A. Magalon, W.R. Hagen, G. Schwarz, Biochemistry 47 (2008) 949.
[23] F. Blasco, J.P. Dos Santos, A. Magalon, C. Frixon, B. Guigliarelli, C.L. Santini, G. Giordano, Mol. Microbiol. 28 (1998) 435.
[24] F. Blasco, J. Pommier, V. Augier, M. Chippaux, G. Giordano, Mol. Microbiol. 6 (1992) 221.
[25] C.S. Chan, J.M. Howell, M.L. Workentine, R.J. Turner, Biochem. Biophys. Res. Commun. 343 (2006) 244.
[26] H. Li, R.J. Turner, Can. J. Microbiol. 55 (2009) 179.
[27] T. Palmer, C.L. Santini, C. Iobbi-Nivol, D.J. Eaves, D.H. Boxer, G. Giordano, Mol. Microbiol. 20 (1996) 875.
[28] J.L. Johnson, N.R. Bastian, K.V. Rajagopalan, Proc. Natl. Acad. Sci. U.S.A. 87 (1990) 3190.
[29] J.L. Johnson, L.W. Indermaur, K.V. Rajagopalan, J. Biol. Chem. 266 (1991) 12140.
[30] J.L. Johnson, K.V. Rajagopalan, Proc. Natl. Acad. Sci. U.S.A. 79 (1982) 6856.
[31] J.C. Hilton, K.V. Rajagopalan, Arch. Biochem. Biophys. 325 (1996) 139.
[32] P.S. Solomon, I. Lane, G.R. Hanson, A.G. McEwan, Eur. J. Biochem. 246 (1997) 200.
[33] K.V. Rajagopalan, J.L. Johnson, J. Biol. Chem. 267 (1992) 10199.
[34] D.P. Kloer, C. Hagel, J. Heider, G.E. Schulz, Structure 14 (2006) 1377.
[35] R.A. Rothery, G.J. Workun, J.H. Weiner, Biochim. Biophys. Acta 1778 (2008) 1897.
[36] H. Schindelin, C. Kisker, J. Hilton, K.V. Rajagopalan, D.C. Rees, Science 272 (1996) 1615.
[37] F. Schneider, J. Löwe, R. Huber, H. Schindelin, C. Kisker, J. Knäblein, J. Mol. Biol. 263 (1996) 53.
[38] J.C. Boyington, V.N. Gladyshev, S.V. Khangulov, T.C. Stadtman, P.D. Sun, Science 275 (1997) 1305.
[39] R. Hille, Chem. Rev. 96 (1996) 2757.
[40] R. Hille, Met. Ions Biol. Syst. 39 (2002) 187.
[41] G.J. Workun, K. Moquin, R.A. Rothery, J.H. Weiner, Microbiol. Mol. Biol. Rev. 72 (2008) 228, table of contents.
[42] M.K. Chan, S. Mukund, A. Kletzin, M.W. Adams, D.C. Rees, Science 267 (1995) 1463.
[43] S. Mukund, M.W. Adams, J. Biol. Chem. 265 (1990) 11508.
[44] J.J. Truglio, K. Theis, S. Leimkühler, R. Rappa, K.V. Rajagopalan, C. Kisker, Structure 10 (2002) 115.
[45] L.E. Bevers, E. Bol, P. Hagedoorn, W.R. Hagen, J. Bacteriol. 187 (2005) 7056.
[46] M. Jormakka, D. Richardson, B. Byrne, S. Iwata, Structure 12 (2004) 95.
[47] C. Kisker, H. Schindelin, A. Pacheco, W.A. Wehbi, R.M. Garrett, K.V. Rajagopalan, J.H. Enemark, D.C. Rees, Cell 91 (1997) 973.
[48] W.H. Campbell, Cell. Mol. Life Sci. 58 (2001) 194.
[49] K. Fischer, G.G. Barbier, H. Hecht, R.R. Mendel, W.H. Campbell, G. Schwarz, Plant Cell 17 (2005) 1167.
[50] E. Bol, N.J. Broers, W.R. Hagen, J. Biol. Inorg. Chem. 13 (2008) 75.
[51] M. Reher, S. Gebhard, P. Schönheit, FEMS Microbiol. Lett. 273 (2007) 196.
[52] J.D. Partridge, D.F. Browning, M. Xu, L.J. Newnham, C. Scott, R.E. Roberts, R.K. Poole, J. Green, Microbiology (Reading Engl.) 154 (2008) 608.
[53] R. Roy, A.L. Menon, M.W. Adams, Methods Enzymol. 331 (2001) 132.
[54] M.J. Romão, M. Archer, I. Moura, J.J. Moura, J. LeGall, R. Engh, M. Schneider, P. Hof, R. Huber, Science 270 (1995) 1170.
[55] R.R. Mendel, F. Bittner, Biochim. Biophys. Acta 1763 (2006) 621.
[56] M. Neumann, G. Mittelstädt, C. Iobbi-Nivol, M. Saggu, F. Lendzian, P. Hildebrandt, S. Leimkühler, FEBS J. 276 (2009) 2762.
[57] I. Bonin, B.M. Martins, V. Purvanov, S. Fetzner, R. Huber, H. Dobbek, Structure 12 (2004) 1425.
[58] M. Bläse, C. Bruntner, B. Tshisuaka, S. Fetzner, F. Lingens, J. Biol. Chem. 271 (1996) 23068.
[59] S. Leimkühler, M. Kern, P.S. Solomon, A.G. McEwan, G. Schwarz, R.R. Mendel, W. Klipp, Mol. Microbiol. 27 (1998) 853.
[60] U. Dietzel, J. Kuper, J.A. Doebbler, A. Schulte, J.J. Truglio, S. Leimkühler, C. Kisker, J. Biol. Chem. 284 (2009) 8768.
[61] B.A. Barata, J. LeGall, J.J. Moura, Biochemistry 32 (1993) 11559.
[62] T. Nishino, K. Okamoto, B.T. Eger, E.F. Pai, T. Nishino, FEBS J. 275 (2008) 3278.
[63] C.C. Page, C.C. Moser, X. Chen, P.L. Dutton, Nature 402 (1999) 47.
[64] C. Kisker, H. Schindelin, D. Baas, J. Rétey, R.U. Meckenstock, P.M. Kroneck, FEMS Microbiol. Rev. 22 (1998) 503.
[65] V. Méjean, C. Iobbi-Nivol, M. Lepelletier, G. Giordano, M. Chippaux, M.C. Pascal, Mol. Microbiol. 11 (1994) 1169.

[66] D.E. Pierson, A. Campbell, J. Bacteriol. 172 (1990) 2194.
[67] S. Dementin, P. Arnoux, B. Frangioni, S. Grosse, C. Léger, B. Burlat, B. Guigliarelli, M. Sabaty, D. Pignol, Biochemistry 46 (2007) 9713.
[68] D. Sambasivarao, R.J. Turner, J.L. Simala-Grant, G. Shaw, J. Hu, J.H. Weiner, J. Biol. Chem. 275 (2000) 22526.
[69] J.H. Weiner, P.T. Bilous, G.M. Shaw, S.P. Lubitz, L. Frost, G.H. Thomas, J.A. Cole, R.J. Turner, Cell 93 (1998) 93.
[70] L.F. Wu, A. Chanal, A. Rodrigue, Arch. Microbiol. 173 (2000) 319.
[71] B.C. Berks, T. Palmer, F. Sargent, Adv. Microb. Physiol. 47 (2003) 187.
[72] J.D. Bendtsen, H. Nielsen, D. Widdick, T. Palmer, S. Brunak, BMC Bioinformatics 6 (2005) 167.
[73] T. Palmer, B.C. Berks, Microbiology (Reading Engl.) 149 (2003) 547.
[74] S.L. McCrindle, U. Kappler, A.G. McEwan, Adv. Microb. Physiol. 50 (2005) 147.
[75] H. Li, K. Temple, K.V. Rajagopalan, H. Schindelin, J. Am. Chem. Soc. (2000) 7673.
[76] L. Zhang, K.J. Nelson, K.V. Rajagopalan, G.N. George, Inorg. Chem. 47 (2008) 1074.
[77] V. Fourmond, B. Burlat, S. Dementin, P. Arnoux, M. Sabaty, S. Boiry, B. Guigliarelli, P. Bertrand, D. Pignol, C. Léger, J. Phys. Chem. B 112 (2008) 15478.
[78] M. Czjzek, J.P. Dos Santos, J. Pommier, G. Giordano, V. Méjean, R. Haser, J. Mol. Biol. 284 (1998) 435.
[79] R.A. Rothery, A. Magalon, G. Giordano, B. Guigliarelli, F. Blasco, J.H. Weiner, J. Biol. Chem. 273 (1998) 7462.
[80] R.A. Rothery, J.L. Grant, J.L. Johnson, K.V. Rajagopalan, J.H. Weiner, J. Bacteriol. 177 (1995) 2057.
[81] P. Arnoux, M. Sabaty, J. Alric, B. Frangioni, B. Guigliarelli, J. Adriano, D. Pignol, Nat. Struct. Biol. 10 (2003) 928.
[82] P.J. Ellis, T. Conrads, R. Hille, P. Kuhn, Structure 9 (2001) 125.
[83] H.D. Thorell, K. Stenklo, J. Karlsson, T. Nilsson, Appl. Environ. Microbiol. 69 (2003) 5585.
[84] E.J. Dridge, C.S. Butler, Biochimie (2010).
[85] C.A. McDevitt, G.R. Hanson, C.J. Noble, M.R. Cheesman, A.G. McEwan, Biochemistry 41 (2002) 15234.
[86] K.S. Bender, C. Shang, R. Chakraborty, S.M. Belchik, J.D. Coates, L.A. Achenbach, J. Bacteriol. 187 (2005) 5090.
[87] L. Potter, H. Angove, D. Richardson, J. Cole, Adv. Microb. Physiol. 45 (2001) 51.
[88] A. Marietou, D. Richardson, J. Cole, S. Mohan, FEMS Microbiol. Lett. 248 (2005) 217.
[89] A. Brigé, D. Leys, T.E. Meyer, M.A. Cusanovich, J.J. Van Beeumen, Biochemistry 41 (2002) 4827.
[90] M.L. Cartron, M.D. Roldán, S.J. Ferguson, B.C. Berks, D.J. Richardson, Biochem. J. 368 (2002) 425.
[91] L.C. Potter, J.A. Cole, Biochem. J. 344 (Pt 1) (1999) 69.
[92] P.J.L. Simpson, D.J. Richardson, R. Codd, Microbiology (Reading Engl.) 156 (2010) 302.
[93] S. Najmudin, P.J. González, J. Trincão, C. Coelho, A. Mukhopadhyay, N.M.F.S.A. Cerqueira, C.C. Romão, I. Moura, J.J.G. Moura, C.D. Brondino, M.J. Romão, J. Biol. Inorg. Chem. 13 (2008) 737.
[94] V. Fourmond, M. Sabaty, P. Arnoux, P. Bertrand, D. Pignol, C. Léger, J. Phys. Chem. B 114 (2010) 3341.
[95] J.H. Weiner, R.A. Rothery, D. Sambasivarao, C.A. Trieber, Biochim. Biophys. Acta 1102 (1992) 1.
[96] F. Blasco, B. Guigliarelli, A. Magalon, M. Asso, G. Giordano, R.A. Rothery, Cell. Mol. Life Sci. 58 (2001) 179.
[97] M. Jormakka, K. Yokoyama, T. Yano, M. Tamakoshi, S. Akimoto, T. Shimamura, P. Curmi, S. Iwata, Nat. Struct. Mol. Biol. 15 (2008) 730.
[98] J.H. Weiner, G. Shaw, R.J. Turner, C.A. Trieber, J. Biol. Chem. 268 (1993) 3238.
[99] W. Dietrich, O. Klimmek, Eur. J. Biochem. 269 (2002) 1086.
[100] A.V. Bogachev, R.A. Murtazina, V.P. Skulachev, J. Bacteriol. 178 (1996) 6233.
[101] M. Jormakka, B. Byrne, S. Iwata, FEBS Lett. 545 (2003) 25.
[102] P. Mitchell, J. Theor. Biol. 62 (1976) 327.
[103] J.J.G. Moura, C.D. Brondino, J. Trincão, M.J. Romão, J. Biol. Inorg. Chem. 9 (2004) 791.
[104] A. Magalon, M. Asso, B. Guigliarelli, R.A. Rothery, P. Bertrand, G. Giordano, F. Blasco, Biochemistry 37 (1998) 7363.
[105] R.A. Rothery, M.G. Bertero, R. Cammack, M. Palak, F. Blasco, N.C.J. Strynadka, J.H. Weiner, Biochemistry 43 (2004) 5324.
[106] J.M. Dias, M.E. Than, A. Humm, R. Huber, G.P. Bourenkov, H.D. Bartunik, S. Bursakov, J. Calvete, J. Caldeira, C. Carneiro, J.J. Moura, I. Moura, M.J. Romão, Structure 7 (1999) 65.
[107] J.W. Peters, W.N. Lanzilotta, B.J. Lemon, L.C. Seefeldt, Science 282 (1998) 1853.
[108] P. Lanciano, A. Savoyant, S. Grimaldi, A. Magalon, B. Guigliarelli, P. Bertrand, J. Phys. Chem. B 111 (2007) 13632.
[109] P. Lanciano, A. Vergnes, S. Grimaldi, B. Guigliarelli, A. Magalon, J. Biol. Chem. 282 (2007) 17468.
[110] R.A. Rothery, M.G. Bertero, T. Spreter, N. Bouromand, N.C.J. Strynadka, J.H. Weiner, J. Biol. Chem. 285 (2010) 8801.
[111] C.C. Page, C.C. Moser, P.L. Dutton, Curr. Opin. Chem. Biol. 7 (2003) 551.
[112] B. Guigliarelli, M. Asso, C. More, V. Augier, F. Blasco, J. Pommier, G. Giordano, P. Bertrand, Eur. J. Biochem. 207 (1992) 61.
[113] B. Guigliarelli, A. Magalon, M. Asso, P. Bertrand, C. Frixon, G. Giordano, F. Blasco, Biochemistry 35 (1996) 4828.
[114] V.W.T. Cheng, E. Ma, Z. Zhao, R.A. Rothery, J.H. Weiner, J. Biol. Chem. 281 (2006) 27662.
[115] J.M. Hudson, K. Heffron, V. Kotlyar, Y. Sher, E. Maklashina, G. Cecchini, F.A. Armstrong, J. Am. Chem. Soc. 127 (2005) 6977.
[116] A. Magalon, D. Lemesle-Meunier, R.A. Rothery, C. Frixon, J.H. Weiner, F. Blasco, J. Biol. Chem. 272 (1997) 25652.
[117] T. Wenz, R. Covian, P. Hellwig, F. Macmillan, B. Meunier, B.L. Trumpower, C. Hunte, J. Biol. Chem. 282 (2007) 3977.
[118] B.E. Schultz, S.I. Chan, Annu. Rev. Biophys. Biomol. Struct. 30 (2001) 23.
[119] S. Grimaldi, R. Arias-Cartin, P. Lanciano, S. Lyubenova, B. Endeward, T.F. Prisner, A. Magalon, B. Guigliarelli, J. Biol. Chem. 285 (2010) 179.
[120] P. Lanciano, A. Magalon, P. Bertrand, B. Guigliarelli, S. Grimaldi, Biochemistry 46 (2007) 5323.
[121] R. Arias-Cartin, S. Lyubenova, P. Ceccaldi, T. Prisner, A. Magalon, B. Guigliarelli, S. Grimaldi, J. Am. Chem. Soc. 132 (2010) 5942.
[122] N. Schrader, K. Fischer, K. Theis, R.R. Mendel, G. Schwarz, C. Kisker, Structure 11 (2003) 1251.
[123] E. Karakas, H.L. Wilson, T.N. Graf, S. Xiang, S. Jaramillo-Busquets, K.V. Rajagopalan, C. Kisker, J. Biol. Chem. 280 (2005) 33506.
[124] U. Kappler, B. Bennett, J. Rethmeier, G. Schwarz, R. Deutzmann, A.G. McEwan, C. Dahl, J. Biol. Chem. 275 (2000) 13202.
[125] H.H. Harris, G.N. George, K.V. Rajagopalan, Inorg. Chem. 45 (2006) 493.
[126] C.J. Doonan, H.L. Wilson, K.V. Rajagopalan, R.M. Garrett, B. Bennett, R.C. Prince, G.N. George, J. Am. Chem. Soc. 129 (2007) 9421.
[127] R.R. Mendel, J. Exp. Bot. 58 (2007) 2289.
[128] R. Hänsch, C. Lang, H. Rennenberg, R.R. Mendel, Plant Biol. (Stuttg) 9 (2007) 589.
[129] R. Hänsch, C. Lang, E. Riebeseel, R. Lindigkeit, A. Gessler, H. Rennenberg, R.R. Mendel, J. Biol. Chem. 281 (2006) 6884.
[130] A. Di Salle, G. D'Errico, F. La Cara, R. Cannio, M. Rossi, Extremophiles 10 (2006) 587.
[131] L. Loschi, S.J. Brokx, T.L. Hills, G. Zhang, M.G. Bertero, A.L. Lovering, J.H. Weiner, N.C.J. Strynadka, J. Biol. Chem. 279 (2004) 50391.
[132] S.J. Brokx, R.A. Rothery, G. Zhang, D.P. Ng, J.H. Weiner, Biochemistry 44 (2005) 10339.
[133] J.A. Maupin-Furlow, J.K. Rosentel, J.H. Lee, U. Deppenmeier, R.P. Gunsalus, K.T. Shanmugam, J. Bacteriol. 177 (1995) 4851.
[134] Miami University, 2010, http://www.ecogene.org/geneinfo.php?eg_id=EG11239.
[135] P.M. McNicholas, S.A. Rech, R.P. Gunsalus, Mol. Microbiol. 23 (1997) 515.
[136] H. Tao, A. Hasona, P.M. Do, L.O. Ingram, K.T. Shanmugam, Arch. Microbiol. 184 (2005) 225.
[137] W.T. Self, A.M. Grunden, A. Hasona, K.T. Shanmugam, Microbiology (Reading Engl.) 145 (Pt 1) (1999) 41.
[138] A.M. Grunden, R.M. Ray, J.K. Rosentel, F.G. Healy, K.T. Shanmugam, J. Bacteriol. 178 (1996) 735.
[139] A. Hasona, W.T. Self, R.M. Ray, K.T. Shanmugam, FEMS Microbiol. Lett. 169 (1998) 111.
[140] P.M. McNicholas, R.C. Chiang, R.P. Gunsalus, Mol. Microbiol. 27 (1998) 197.
[141] C. Constantinidou, J.L. Hobman, L. Griffiths, M.D. Patel, C.W. Penn, J.A. Cole, T.W. Overton, J. Biol. Chem. 281 (2006) 4802.
[142] H. Körner, H.J. Sofia, W.G. Zumft, FEMS Microbiol. Rev. 27 (2003) 559.
[143] J. Green, J.C. Crack, A.J. Thomson, N.E. LeBrun, Curr. Opin. Microbiol. 12 (2009) 145.
[144] G. Unden, S. Achebach, G. Holighaus, H.G. Tran, B. Wackwitz, Y. Zeuner, J. Mol. Microbiol. Biotechnol. 4 (2002) 263.
[145] J. Crack, J. Green, A.J. Thomson, J. Biol. Chem. 279 (2004) 9278.
[146] E.L. Mettert, P.J. Kiley, J. Bacteriol. 189 (2007) 3036.
[147] R.P. Gunsalus, S.J. Park, Res. Microbiol. 145 (1994) 437.
[148] K.A. Salmon, S. Hung, N.R. Steffen, R. Krupp, P. Baldi, G.W. Hatfield, R.P. Gunsalus, J. Biol. Chem. 280 (2005) 15084.
[149] R. Malpica, B. Franco, C. Rodriguez, O. Kwon, D. Georgellis, Proc. Natl. Acad. Sci. U.S.A. 101 (2004) 13318.
[150] D. Georgellis, O. Kwon, E.C. Lin, Science 292 (2001) 2314.
[151] V. Stewart, Biochem. Soc. Trans. 31 (2003) 1.
[152] C.E. Noriega, H. Lin, L. Chen, S.B. Williams, V. Stewart, Mol. Microbiol. 75 (2010) 394.
[153] L.V. Kalman, R.P. Gunsalus, J. Bacteriol. 172 (1990) 7049.
[154] S.M.D. Bearson, J.A. Albrecht, R.P. Gunsalus, BMC Microbiol. 2 (2002) 13.
[155] G. Simon, V. Méjean, C. Jourlin, M. Chippaux, M.C. Pascal, J. Bacteriol. 176 (1994) 5601.
[156] C. Jourlin, A. Bengrine, M. Chippaux, V. Méjean, Mol. Microbiol. 20 (1996) 1297.
[157] C. Baraquet, L. Théraulaz, M. Guiral, D. Lafitte, V. Méjean, C. Jourlin-Castelli, J. Biol. Chem. 281 (2006) 38189.
[158] M. Ansaldi, L. Théraulaz, V. Méjean, Proc. Natl. Acad. Sci. U.S.A. 101 (2004) 9423.
[159] S. Gon, C. Jourlin-Castelli, L. Théraulaz, V. Méjean, Proc. Natl. Acad. Sci. U.S.A. 98 (2001) 11615.
[160] A. Serganov, D.J. Patel, Biochim. Biophys. Acta 1789 (2009) 592.
[161] E.E. Regulski, R.H. Moy, Z. Weinberg, J.E. Barrick, Z. Yao, W.L. Ruzzo, R.R. Breaker, Mol. Microbiol. 68 (2008) 918.
[162] M.J. Romao, Dalton Trans. (2009) 4053.
[163] N.M.F.S.A. Cerqueira, P.J. Gonzalez, C.D. Brondino, M.J. Romão, C.C. Romão, I. Moura, J.J.G. Moura, J. Comput. Chem. 30 (2009) 2466.
[164] P. Tavares, A. Pereira, J. Moura, I. Moura, J. Inorg. Biochem. 100 (2006) 2087.
[165] J.F. Stolz, P. Basu, J.M. Santini, R.S. Oremland, Annu. Rev. Microbiol. 60 (2006) 107.
[166] R.M. Martinez-Espinosa, E.J. Dridge, M.J. Bonete, J.N. Butt, C.S. Butler, F. Sargent, D.J. Richardson, FEMS Microbiol. Lett. 276 (2007) 129.

[167] E.C. Lowe, S. Bydder, R.S. Hartshorne, H.L.U. Tape, E.J. Dridge, C.M. Debieux, K. Paszkiewicz, I. Singleton, R.J. Lewis, J.M. Santini, D.J. Richardson, C.S. Butler, J. Biol. Chem. 285 (2010) 18433.
[168] J. Simon, R.J.M. van Spanning, D.J. Richardson, Biochim. Biophys. Acta 1777 (2008) 1480.
[169] A.S. McAlpine, A.G. McEwan, S. Bailey, J. Mol. Biol. 275 (1998) 613.
[170] J.M. Rebelo, J.M. Dias, R. Huber, J.J. Moura, M.J. Romão, J. Biol. Inorg. Chem. 6 (2001) 791.
[171] A. Messerschmidt, H. Niessen, D. Abt, O. Einsle, B. Schink, P.M.H. Kroneck, Proc. Natl. Acad. Sci. U.S.A. 101 (2004) 11571.
[172] M. Unciuleac, E. Warkentin, C.C. Page, M. Boll, U. Ermler, Structure 12 (2004) 2249.
[173] C.P. Witte, M.I. Igeño, R. Mendel, G. Schwarz, E. Fernández, FEBS Lett. 431 (1998) 205.
[174] T. Kruse, C. Gehl, M. Geisler, M. Lehrke, P. Ringel, S. Hallier, R. Hänsch, R.R. Mendel, J. Biol. Chem. 285 (2010) 6623.
[175] A. Magalon, C. Frixon, J. Pommier, G. Giordano, F. Blasco, J. Biol. Chem. 277 (2002) 48199.
[176] A. Vergnes, K. Gouffi-Belhabich, F. Blasco, G. Giordano, A. Magalon, J. Biol. Chem. 279 (2004) 41398.
[177] C.A. Temple, K.V. Rajagopalan, J. Biol. Chem. 275 (2000) 40202.
[178] M. Ilbert, V. Méjean, M. Giudici-Orticoni, J. Samama, C. Iobbi-Nivol, J. Biol. Chem. 278 (2003) 28787.
[179] M. Neumann, M. Schulte, N. Jünemann, W. Stöcklein, S. Leimkühler, J. Biol. Chem. 281 (2006) 15701.
[180] C.E. Price, A.J.M. Driessen, J. Biol. Chem. 283 (2008) 26921.
[181] J.A. Gralnick, H. Vali, D.P. Lies, D.K. Newman, Proc. Natl. Acad. Sci. U.S.A. 103 (2006) 4669.
[182] F. Sargent, Biochem. Soc. Trans. 35 (2007) 835.
[183] H. Li, L. Chang, J.M. Howell, R.J. Turner, Biochim. Biophys. Acta (BBA): Proteins Proteomic. 1804 (2010) 1301.
[184] C.F.R.O. Matos, A. Di Cola, C. Robinson, EMBO Rep. 10 (2009) 474.
[185] C.F.R.O. Matos, C. Robinson, A. Di Cola, EMBO J. 27 (2008) 2055.
[186] U. Lindenstrauss, C.F.R.O. Matos, W. Graubner, C. Robinson, T. Brüser, FEBS Lett. 584 (2010) 3644.
[187] F. Blasco, F. Nunzi, J. Pommier, R. Brasseur, M. Chippaux, G. Giordano, Mol. Microbiol. 6 (1992) 209.
[188] O. Kirillova, M. Chruszcz, I.A. Shumilin, T. Skarina, E. Gorodichtchenskaia, M. Cymborowski, A. Savchenko, A. Edwards, W. Minor, Acta Crystallogr. D Biol. Crystallogr. 63 (2007) 348.
[189] S. Tranier, C. Iobbi-Nivol, C. Birck, M. Ilbert, I. Mortier-Barrière, V. Méjean, J. Samama, Structure 11 (2003) 165.
[190] Y. Qiu, R. Zhang, T.A. Binkowski, V. Tereshko, A. Joachimiak, A. Kossiakoff, Proteins 71 (2008) 525.
[191] S.K. Ramasamy, W.M. Clemons, Acta Crystallogr. Sect. F Struct. Biol. Cryst. Commun. 65 (2009) 746.
[192] S. Zakian, D. Lafitte, A. Vergnes, C. Pimentel, C. Sebban-Kreuzer, R. Toci, J. Claude, F. Guerlesquin, A. Magalon, FEBS J. 277 (2010) 1886.
[193] A. Vergnes, J. Pommier, R. Toci, F. Blasco, G. Giordano, A. Magalon, J. Biol. Chem. 281 (2006) 2170.
[194] R.L. Jack, G. Buchanan, A. Dubini, K. Hatzixanthis, T. Palmer, F. Sargent, EMBO J. 23 (2004) 3962.
[195] R.J. Turner, A.L. Papish, F. Sargent, Can. J. Microbiol. 50 (2004) 225.
[196] B. Ize, S.J. Coulthurst, K. Hatzixanthis, I. Caldelari, G. Buchanan, E.C. Barclay, D.J. Richardson, T. Palmer, F. Sargent, Microbiology (Reading Engl.) 155 (2009) 3992.
[197] T.L. Winstone, M.L. Workentine, K.J. Sarfo, A.J. Binding, B.D. Haslam, R.J. Turner, Arch. Biochem. Biophys. 455 (2006) 89.
[198] D. Guymer, J. Maillard, M.F. Agacan, C.A. Brearley, F. Sargent, FEBS J. 277 (2010) 511.
[199] P. Hänzelmann, H. Dobbek, L. Gremer, R. Huber, O. Meyer, J. Mol. Biol. 301 (2000) 1221.
[200] I.J. Oresnik, C.L. Ladner, R.J. Turner, Mol. Microbiol. 40 (2001) 323.
[201] D. Guymer, J. Maillard, F. Sargent, Arch. Microbiol. 191 (2009) 519.
[202] C.S. Chan, L. Chang, K.L. Rommens, R.J. Turner, J. Bacteriol. 191 (2009) 2091.
[203] C.M. Stevens, T.M.L. Winstone, R.J. Turner, M. Paetzel, J. Mol. Biol. 389 (2009) 124.
[204] J.S. Kostecki, H. Li, R.J. Turner, M.P. DeLisa, PLoS ONE 5 (2010) e9225.
[205] A.L. Papish, C.L. Ladner, R.J. Turner, J. Biol. Chem. 278 (2003) 32501.
[206] C.S. Chan, T.M.L. Winstone, L. Chang, C.M. Stevens, M.L. Workentine, H. Li, Y. Wei, M.J. Ondrechen, M. Paetzel, R.J. Turner, Biochemistry 47 (2008) 2749.
[207] K. Hatzixanthis, T.A. Clarke, A. Oubrie, D.J. Richardson, R.J. Turner, F. Sargent, Proc. Natl. Acad. Sci. U.S.A. 102 (2005) 8460.
[208] I. Schröder, S. Rech, T. Krafft, J.M. Macy, J. Biol. Chem. 272 (1997) 23765.
[209] O. Kniemeyer, J. Heider, Arch. Microbiol. 176 (2001) 129.
[210] S. Duval, A. Ducluzeau, W. Nitschke, B. Schoepp-Cothenet, BMC Evol. Biol. 8 (2008) 206.
[211] H.G. Enoch, R.L. Lester, J. Biol. Chem. 250 (1975) 6693.
[212] F. Zinoni, A. Birkmann, T.C. Stadtman, A. Böck, Proc. Natl. Acad. Sci. U.S.A. 83 (1986) 4650.
[213] M.A. Mandrand-Berthelot, G. Couchoux-Luthaud, C.L. Santini, G. Giordano, J. Gen. Microbiol. 134 (1988) 3129.
[214] J. Pommier, M.A. Mandrand, S.E. Holt, D.H. Boxer, G. Giordano, Biochim. Biophys. Acta 1107 (1992) 305.
[215] C. Schlindwein, G. Giordano, C.L. Santini, M.A. Mandrand, J. Bacteriol. 172 (1990) 6112.
[216] V. Stewart, J.T. Lin, B.L. Berg, J. Bacteriol. 173 (1991) 4417.
[217] I. Lüke, G. Butland, K. Moore, G. Buchanan, V. Lyall, S.A. Fairhurst, J.F. Greenblatt, A. Emili, T. Palmer, F. Sargent, Arch. Microbiol. 190 (2008) 685.
[218] G. Butland, J.M. Peregrín-Alvarez, J. Li, W. Yang, X. Yang, V. Canadien, A. Starostine, D. Richards, B. Beattie, N. Krogan, M. Davey, J. Parkinson, J. Greenblatt, A. Emili, Nature 433 (2005) 531.
[219] J. Maillard, C.A.E.M. Spronk, G. Buchanan, V. Lyall, D.J. Richardson, T. Palmer, G.W. Vuister, F. Sargent, Proc. Natl. Acad. Sci. U.S.A. 104 (2007) 15641.
[220] A. Nilavongse, T.H.C. Brondijk, T.W. Overton, D.J. Richardson, E.R. Leach, J.A. Cole, Microbiology (Reading Engl.) 152 (2006) 3227.
[221] M.F. Olmo-Mira, M. Gavira, D.J. Richardson, F. Castillo, C. Moreno-Vivián, M.D. Roldán, J. Biol. Chem. 279 (2004) 49727.
[222] M. Kern, J. Simon, Microbiology (Reading Engl.) 155 (2009) 2784.
[223] A. Silvestro, J. Pommier, M.C. Pascal, G. Giordano, Biochim. Biophys. Acta 999 (1989) 208.
[224] J. Pommier, V. Méjean, G. Giordano, C. Iobbi-Nivol, J. Biol. Chem. 273 (1998) 16615.
[225] O. Genest, M. Ilbert, V. Méjean, C. Iobbi-Nivol, J. Biol. Chem. 280 (2005) 15644.
[226] A.L. Shaw, S. Leimkuhler, W. Klipp, G.R. Hanson, A.G. McEwan, Microbiology (Reading Engl.) 145 (Pt 6) (1999) 1409.
[227] S. Tranier, I. Mortier-Barrière, M. Ilbert, C. Birck, C. Iobbi-Nivol, V. Méjean, J. Samama, Protein Sci. 11 (2002) 2148.
[228] O. Genest, M. Neumann, F. Seduk, W. Stöcklein, V. Méjean, S. Leimkühler, C. Iobbi-Nivol, J. Biol. Chem. 283 (2008) 21433.
[229] O. Genest, F. Seduk, L. Théraulaz, V. Méjean, C. Iobbi-Nivol, FEMS Microbiol. Lett. 265 (2006) 51.
[230] M. Ilbert, V. Méjean, C. Iobbi-Nivol, Microbiology (Reading Engl.) 150 (2004) 935.
[231] F. Bittner, M. Oreb, R.R. Mendel, J. Biol. Chem. 276 (2001) 40381.
[232] M. Neumann, W. Stöcklein, A. Walburger, A. Magalon, S. Leimkühler, Biochemistry 46 (2007) 9586.
[233] S. Leimkühler, W. Klipp, J. Bacteriol. 181 (1999) 2745.
[234] S. Schumann, M. Saggu, N. Möller, S.D. Anker, F. Lendzian, P. Hildebrandt, S. Leimkühler, J. Biol. Chem. 283 (2008) 16602.
[235] L. Gremer, O. Meyer, Eur. J. Biochem. 238 (1996) 862.
[236] P. Sachelaru, E. Schiltz, R. Brandsch, Appl. Environ. Microbiol. 72 (2006) 5126.
[237] F. Baymann, E. Lebrun, M. Brugna, B. Schoepp-Cothenet, M. Giudici-Orticoni, W. Nitschke, Philos. Trans. R. Soc. Lond. B Biol. Sci. 358 (2003) 267.
[238] F. Sargent, Microbiology (Reading Engl.) 153 (2007) 633.
[239] B.S. Kang, Y.M. Kim, J. Bacteriol. 181 (1999) 5581.
[240] J. Rebelo, S. Macieira, J.M. Dias, R. Huber, C.S. Ascenso, F. Rusnak, J.J. Moura, I. Moura, M.J. Romão, J. Mol. Biol. 297 (2000) 135.
[241] Y. Hu, S. Faham, R. Roy, M.W. Adams, D.C. Rees, J. Mol. Biol. 286 (1999) 899.
[242] Q. Xiang, D.E. Edmondson, Biochemistry 35 (1996) 5441.
[243] H. Dalton, D.J. Lowe, T. Pawlik, R.C. Bray, Biochem. J. 153 (1976) 287.
[244] M. Resch, H. Dobbek, O. Meyer, J. Biol. Inorg. Chem. 10 (2005) 518.
[245] C. Feng, U. Kappler, G. Tollin, J.H. Enemark, J. Am. Chem. Soc. 125 (2003) 14696.
[246] K. Johnson-Winters, G. Tollin, J.H. Enemark, Biochemistry 49 (2010) 7242.
[247] U. Kappler, S. Bailey, J. Biol. Chem. 280 (2005) 24999.
[248] U. Kappler, S. Bailey, Acta Crystallogr. D Biol. Crystallogr. 60 (2004) 2070.
[249] K. Aguey-Zinsou, P.V. Bernhardt, U. Kappler, A.G. McEwan, J. Am. Chem. Soc. 125 (2003) 530.
[250] B.C. Berks, S.J. Ferguson, J.W. Moir, D.J. Richardson, Biochim. Biophys. Acta 1232 (1995) 97.
[251] G.B. Seiffert, G.M. Ullmann, A. Messerschmidt, B. Schink, P.M.H. Kroneck, O. Einsle, Proc. Natl. Acad. Sci. U.S.A. 104 (2007) 3073.
[252] R.N. vanden Hoven, J.M. Santini, Biochim. Biophys. Acta 1656 (2004) 148.
[253] B.J.N. Jepson, S. Mohan, T.A. Clarke, A.J. Gates, J.A. Cole, C.S. Butler, J.N. Butt, A.M. Hemmings, D.J. Richardson, J. Biol. Chem. 282 (2007) 6425.
[254] N.K. Heinzinger, S.Y. Fujimoto, M.A. Clark, M.S. Moreno, E.L. Barrett, J. Bacteriol. 177 (1995) 2813.
[255] D.J. Richardson, N.J. Watmough, Curr. Opin. Chem. Biol. 3 (1999) 207.
[256] W.L. DeLano, The PyMOL Molecular Graphics System, Schrödinger, LLC, 2002.